frontiers | Frontiers in Chemical Engineering

TYPE Review
PUBLISHED 16 September 2022
DOI 10.3389/fceng.2022.995221

Check for updates

OPEN ACCESS

EDITED BY
Colin Hare,
Newcastle University, United Kingdom

REVIEWED BY
Alejandro López,
University of Deusto, Spain
Edward Garboczi,
National Institute of Standards and Technology (NIST), United States
Yusheng Shi,
Huazhong University of Science and Technology, China

*CORRESPONDENCE
Jochen Schmidt,
jochen.schmidt@fau.de

SPECIALTY SECTION
This article was submitted to Materials Process Engineering, a section of the journal Frontiers in Chemical Engineering

RECEIVED 15 July 2022
ACCEPTED 25 August 2022
PUBLISHED 16 September 2022

CITATION
Schmidt J and Peukert W (2022), Dry powder coating in additive manufacturing.
*Front. Chem. Eng.* 4:995221.
doi: 10.3389/fceng.2022.995221

COPYRIGHT
© 2022 Schmidt and Peukert. This is an open-access article distributed under the terms of the Creative Commons Attribution License (CC BY). The use, distribution or reproduction in other forums is permitted, provided the original author(s) and the copyright owner(s) are credited and that the original publication in this journal is cited, in accordance with accepted academic practice. No use, distribution or reproduction is permitted which does not comply with these terms.

# Dry powder coating in additive manufacturing

Jochen Schmidt[1,2]* and Wolfgang Peukert[1,2]

[1]Department of Chemical and Biological Engineering, Institute of Particle Technology, Friedrich-Alexander-Universität Erlangen-Nürnberg, Erlangen, Germany, [2]Interdisciplinary Center for Functional Particle Systems, Friedrich-Alexander-Universität Erlangen-Nürnberg, Erlangen, Germany

Dry powder coating is used in many industries to tailor the bulk solid characteristics of cohesive powders. Within this paper, the state of the art of dry coating of feedstock materials for powder based additive manufacturing (AM) processes will be reviewed. The focus is on feedstock materials for powder bed fusion AM processes, such as powder bed fusion of polymers with a laser beam and powder bed fusion of metals with lasers or an electron beam. Powders of several microns to several ten microns in size are used and the feedstock's bulk solid properties, especially the flowability and packing density are of immanent importance in different process steps in particular for powder dosing and spreading of powder layers onto the building area. All these properties can be tuned by dry particle coating. Moreover, possibilities to improve AM processability and to manipulate the resulting microstructure (c.f. grain refinement, dispersion strengthening) by adhering nanoparticles on the powders will be discussed. The effect of dry coating on the obtained powder properties along the whole AM process chain and the resulting part properties is assessed. Moreover, appropriate characterization methods for bulk solid properties of dry-coated AM powders are critically discussed.

KEYWORDS

**powder bed fusion, selective laser sintering, selective laser melting, dry coating, nanoparticles, bulk solid properties, flowability, microstructure**

## 1 Introduction

In many industries and applications particles in the size range below 100 µm are relevant either as a final or as an intermediate product. In this size range, particle-particle interactions, especially the interparticulate van der Waals (vdW) forces determine the behavior of the particle system, as they exceed the gravitational forces by many orders of magnitude (Rumpf, 1974; Israelachvili, 2011). In consequence, these fine powders typically are more cohesive the finer they get and characterized by poor flowability and often low bulk density, which poses considerable challenges during handling, storage and dosing. To improve the flowability of cohesive powders, such as e.g. pharmaceutical, food products, toner systems or powders for additive manufacturing (AM), dry particle coating with flowing aids is frequently applied (Pfeffer et al., 2001; Zhou et al., 2003; Zimmermann et al., 2004; Yang et al., 2005; Bose and Bogner, 2007; Tomas and Kleinschmidt, 2009; Blümel et al., 2015; Schmidt et al., 2016b; Kusoglu et al., 2021; Lüddecke et al., 2021). Dry particle coating for surface functionalization is not limited to

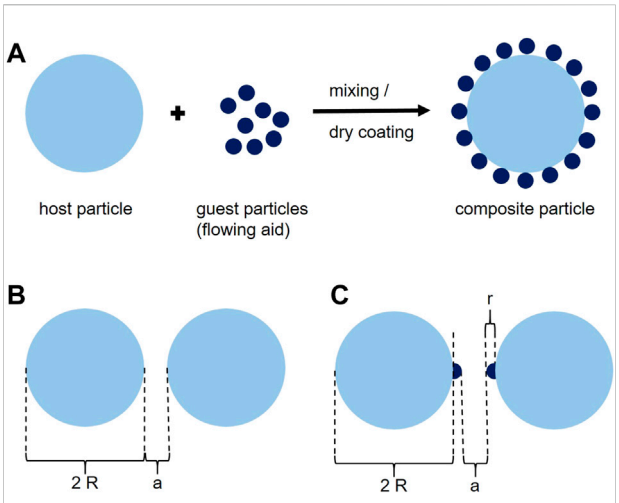


FIGURE 1
**(A)** formation of composite particles by dry particle coating of host particles with nanoscale guest particles, **(B)** geometry for description of vdW interactions between two spheres of identical size according to Eq. 1, **(C)** geometry for description of vdW interactions between two spheres with asperity or radius of curvature according to Eq. 2 (Rumpf, 1974).

the application of flow enhancers. One can think of many more types of surface functionalization including coloring and, thus, tailoring of the absorption behavior (Jadhav et al., 2019; Jadhav et al., 2020; Jadhav et al., 2021; Lüddecke et al., 2021; Pannitz et al., 2021), charge control (Düsenberg et al., 2022a; Düsenberg et al., 2022b), improvement of electrical conductivity (Blümel et al., 2014), tuning the performance of batteries (Cho and Cho, 2010) or tailoring the dissolution behavior (Linsenbühler and Wirth, 2005), to only name a few examples. Within this paper, we will review recent advances in the application of dry powder coating processes for modification of AM powders with a focus on feedstock materials for powder bed fusion (PBF), i.e., PBF of polymers with a laser beam (PBF-LB/P) and PBF of metals with a laser or electron beam (PBF-LB/M, PBF-EB/M). Dry powder coating offers many possibilities to tune the AM feedstock powder's processability with positive effects on the resulting manufactured part properties. In PBF-AM, bulk solid properties of the feedstock material, which are typically particles in the size range of several 10 microns, are essential. Especially AM polymer powders may exhibit a cohesive behavior impairing their flowability and packing density. The processability of such powders can be considerably improved by the functionalization of the particles' surfaces by adhesion of nanoparticles acting as flowing aids by dry coating. Moreover, dry coating also offers the possibility to tune the laser absorption of the powder feedstock and the microstructure of the manufactured part. The effect of dry coating on the obtained powders' properties along the whole AM process chain from powder production to resulting part properties will be assessed.

In the following, we give a brief introduction into the dry particle coating process, prior to discussing applications of dry coating in AM.

## 1.1 Dry particle coating

In dry powder coating, surface functionalized, nano-rough composite particles are obtained by mixing host particles with nanoscale guest particles (Figure 1A). The host particles typically are of several microns up to 200 microns size (Pfeffer et al., 2001). The guest particles adhere onto the host particles' surfaces due to vdW interactions. By formation of composite particles, i.e., adhesion of nanoparticles acting as asperities on the host microparticles, the total vdW particle-particle interaction forces are considerably reduced (Zhou et al., 2003) and, thus, flowability is enhanced. The schematic in Figure 1A depicts coating of host particles with individual guest nanoparticles e.g., by coating of microparticles in the gas phase with *in situ* formed nanoparticles (Gómez Bonilla et al., 2021a). However, if dry coating is performed with fumed oxides, the added guest particles are mostly agglomerated. In this case, the nanoparticles must be sufficiently dispersed before or during the coating process. A more detailed description of these mechanism is given in (Alonso et al., 1988; Pfeffer et al., 2001; Düsenberg et al., 2022b).

For dry powder coating any device can be used that provides a certain minimum stressing energy allowing for de-agglomeration of the host and guest particles and a sufficiently high number of collisions to realize a homogeneous coating. Thus, mixers (high-energy mixers, tumbling mixers), grinding equipment, such as ball or planetary ball mills, but also impact mills and fluidized beds have been applied for dry powder coating (Pfeffer et al., 2001). Depending on the acting stresses and number of collisions, different types of surface functionalization can be realized. The host particles may be decorated with guest particles only bound to the host particles surfaces by interparticulate forces. This is achieved for instance in fluidized bed coating, or in tumbling mixers for moderate process times (Blümel, 2015; Blümel et al., 2015). In contrast, the guest may also be fused into the host particle surface upon applying strong shear and normal forces during coating, like in hybridization (Nara Machinery) or mechanofusion (Hosokawa) systems (Yokoyama et al., 1987; Naito et al., 1993).

An extensive discussion of flow enhancers, their action and models to describe their effect and that of surface roughness on particle interactions may be found e.g. in (Zhou et al., 2003; Zimmermann et al., 2004; Tomas and Kleinschmidt, 2009; Gärtner et al., 2021).

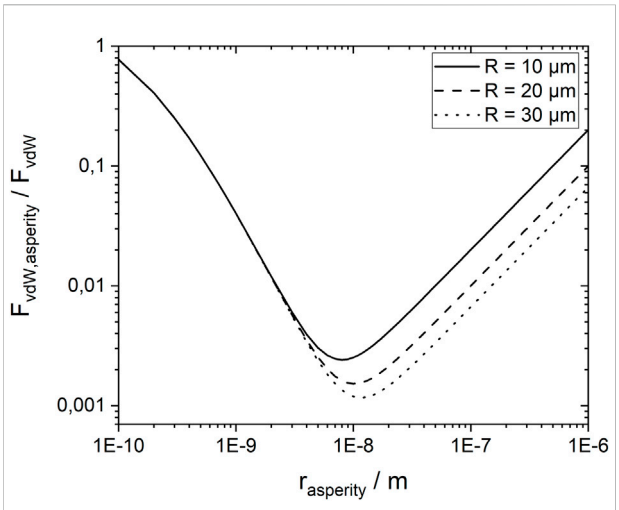


FIGURE 2
vdW interaction force $F_{vdW,asperity}$ between two particles of radius R at contact (contact distance: 0.165 nm) due to an asperity of radius of curvature r (cf. Figures 1B,C) relative to the vdW force interaction between two particles without asperity, $F_{vdW}$, according to Rumpf (Rumpf, 1974).

The vdW interaction force $F_{vdW}$ between two (host) particles of radius R of the same material (Figure 1B) may be written as

$$F_{vdW} = -\frac{A_H}{6 \cdot a^2} \cdot \frac{R^2}{2 \cdot R} \quad (1)$$

$A_H$ is the Hamaker constant, a the interparticle distance. By adhering nanoparticles onto the host particles, composite particles with asperities characterized by a radius of curvature r are formed (see Figure 1C). In this case, the vdW interaction force $F_{vdW,\ asperity}$ between two particles of same size and material with an asperity, is given in the model by Rumpf (1974) as

$$F_{vdW,\ asperity} = -\frac{A_H}{6} \cdot \left( \frac{R}{(a+r)^2} + \frac{r}{a^2} \right) \quad (2)$$

The effect of the radius of asperity r on vdW interactions between two host particles of radius R expressed as the dimensionless vdW force $\frac{F_{vdW,\ asperity}}{F_{vdW}}$ at a minimum contact distance of 0.165 nm (Israelachvili, 2011) is exemplified in Figure 2 for host particles of 10 µm, 20 and 30 µm radius. A minimum in the dimensionless vdW force is observed for asperities with radii of curvature of several 10 nanometers. Thus, nanoscale flowing aids in this size range allow to reduce the adhesion forces of the host materials by several orders of magnitude (Zimmermann et al., 2004; Tomas and Kleinschmidt, 2009; Blümel et al., 2015; Gärtner et al., 2021).

Adhesion forces in technical systems are typically widely distributed due to varying particle sizes and shapes, roughness, impurities and adsorbed layers. Any in-depth analysis of adhesion forces must therefore consider adhesion force distributions. Götzinger and Peukert (Götzinger and Peukert, 2004) identified three types of such distributions: mono- and bimodal Weibull distributions and lognormal distributions for systems of widely distributed contact geometries. Such distributions can easily span one or two orders of magnitude. The validity of Weibull distributions implies that adhesion is related to breakage, i.e. the adhesive bond must be broken to separate the contact partners: This occurs in any measurement of the adhesion force. The minimal adhesion force occurs in a situation where the density in the contact region is minimal, for instance in the point contact between two asperities. The adhesion is maximal in a situation where the contact density is maximal. This case refers to close packing of the roughness asperities or by viscous or plastic deformation during adhesion and compaction (Zhou and Peukert, 2008). The latter leads to adhesion force hysteresis due to irreversible deformation upon contact, which is particularly pronounced for soft polymer powders.

The influence of humidity is complex. At low humidity the condensed water layers are thin (a monolayer or just a few layers) and can be immobile and even ice-like. In this case, the Hamaker constant is changed by the adsorbed layer and surface conductivity increases reducing unwanted effects of electrification and charge accumulation. At increased humidity, water layers get thicker and mobile, pore condensation may induce neck formation at the contact between the particles. These effects lead to a strong increase of adhesion forces by liquid bridges and thus to enhanced cohesion in powder flow and reduced packing densities.

## 1.2 Additive manufacturing technologies

Additive manufacturing (AM) is a collective term summarizing different processes allowing for manufacturing of parts from layered, viscous or powdery materials without shaping tools. AM offers a large freedom in design, thus, complex geometries are accessible that are hard (or impossible) to produce by conventional (subtractive) manufacturing. The increasing interest in AM for production of functional parts in industry and in academia over the last decade is reflected by the increasing number of publications with respect to material development for AM processes, feedstock characterization or design criteria for AM parts. Irrespective of the type of feedstock material used, AM technologies can be sub-divided into seven process categories according to ISO/ASTM 52900, namely material extrusion (MEX), material jetting (MJT), binder jetting (BJT), vat photopolymerization (VPP), powder bed fusion (PBF), sheet lamination (SHL) and directed energy deposition (DED). In case of plastic components MEX and PBF are so far the only applicable options for production of functional parts of sufficient mechanical properties. Concerning functional parts built from metal feedstocks, PBF and DED can be applied. If functional ceramic components are desired, green bodies can be produced, for example, via MEX, BJT or PBF.

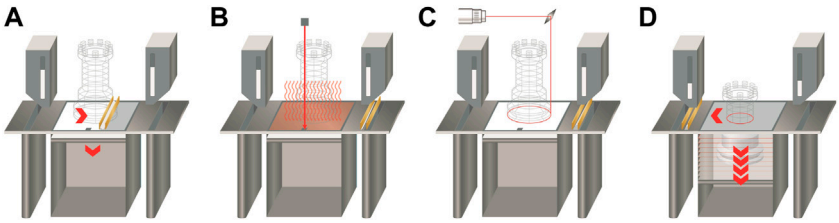


FIGURE 3
Process steps in PBF-LB/P: **(A)** dosing of feedstock from the hopper and subsequent powder deposition by a rake, **(B)** heating of newly applied powder layer by IR heaters (control *via* a pyrometer), **(C)** selective fusion of the powder according to the contour of the component by a laser, **(D)** lowering of building platform. The process steps **(A)** to **(D)** are repeated until the part is complete (adapted from EOS).

Concerning single-stage AM processes, PBF is the method of choice to manufacture functional components using metal, plastic, as well as composite powder feedstocks. The currently employed PBF processes for polymers and metals use a laser, respectively, a laser or an electron gun as beam source. According to the standard terminology of AM technologies, the respective processes are PBF of polymers with laser beam (PBF-LB/P), PBF of metals with laser beam (PBF-LB/M) and PBF of metals with electron beam (PBF-EB/M).

In these PBF processes, particle handling is of immanent importance, as feedstock materials of good flowability, spreadability and high and homogeneous packing density are needed to produce dense components of accurate geometry and sufficient mechanical strength. Bulk solid characteristics in the context of AM have been referred to as "non-intrinsic or extrinsic material properties," i.e. characteristics tuned during pre-processing or production of a feedstock that do not depend on the chemical structure of e.g. a polymer or the chemical composition. They are contrasted by "intrinsic material properties" like absorptivity, melt viscosity or thermal properties (melting temperature, mass-specific melting enthalpy etc.) depending on the chemical structure or the composition, but not being dependent on the amount of the material or its dispersed state (Amado et al., 2011; Schmid, 2018). A frequently applied approach to improve bulk solid properties of AM powders is dry coating (Dechet et al., 2019). Dry particle coating allows to produce novel composite particle systems and, thus, e.g. to tune the absorption behavior of the powder (Pannitz et al., 2021) or the phase morphology of the part (Mair et al., 2021). This article reviews the state of the art of dry particle coating for functionalization of powder feedstocks in PBF-AM with a focus on applications in PBF-LB/P and PBF-LB/M.

## 1.3 Powder bed fusion additive manufacturing

In the following, the process steps and the importance of particle and bulk solid properties of the feedstocks will be sketched exemplarily for PBF-LB/P. In this process, the component is manufactured layer by layer in a powder bed. A sketch of the building chamber of a commercial PBF machine and the process cycle are depicted in Figure 3.

The heated building chamber is flushed with nitrogen and includes a movable building platform and a powder spreading unit, which can be e.g. a roller coater or a rake. The building chamber is tempered by infrared heaters attached to the top of the building chamber that illuminate the building area. The building chamber temperature typically is 20 K below the melting temperature of the feedstock. In case of processing of polyamide 12 (PA12) it is close to 170°C. The polymer powder feedstock is stored in hoppers that e.g. are arranged to the top left and top right of the building platform.

i) In a first step (Figure 3A), powder is released from the hopper, and a thin powder layer of typically 100–150 µm is deposited onto the building platform by means of the spreading unit, c.f. the rake depicted in yellow.
ii) The IR heaters are switched on to heat the newly applied powder layer in the building area; temperature is controlled by a pyrometer (Figure 3B). Ideally, a homogeneous powder layer of smooth surface and uniform packing fraction along the building area is desired. The over-flow powder, i.e. the excess amount of powder not needed to form the powder layer, is collected in overflow bins, which are situated on the bottom left and bottom right of the building platform.
iii) The part contours of the final component to be built in this layer are 'written' into the powder layer by means of a laser spot (Figure 3C). For this purpose, in PBF-LB/P typically $CO_2$ lasers (10.6 µm wavelength) are employed. The laser spot is focused into the xy building plane and guided via galvo scanners. In the illuminated area, the plastic feedstock powder is converted to melt.
iv) The building platform is lowered (Figure 3D) and the process is repeated from step (A). After the building job is finished, the heating is switched off and the setup cools down.

During cooling, the final solid part forms due to solidification and crystallization of the melt. Finally, the PBF-LB/P-built parts

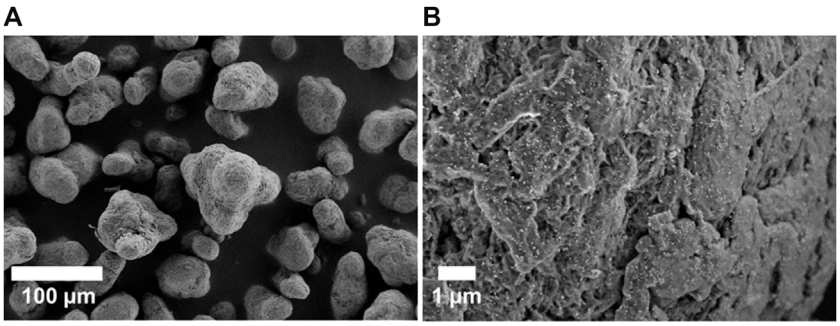


FIGURE 4
**(A)** SEM images of a PA12 PBF-LB/P feedstock powder (PA2200, EOS), **(B)** surface detail of a PA12 particle showing silica nanoparticles adhered as flowing aid.

are separated from the powder bed ("part cake") and subjected to post-processing. The general process steps in PBF-LB/M are almost identical to that in PBF-LB/P; depending on the feedstock material other inert gases with lower oxygen impurity levels are necessary. In PBF-LB/M the molten areas solidify again prior to spreading of the next powder layer in contrast to the situation in PBF-LB/P, where it is inevitable for proper manufacture that the illuminated areas stay in the molten state until the next powder layer is spread and illuminated. In PBF-EB/M a major difference is that the process is performed under vacuum conditions and that the whole building area is illuminated (at reduced intensity) to sinter the particles and, thus, allow for proper electric conductivity of the bed prior to writing the part contours and cross sections with the electron beam.

The most important powder bulk properties for PBF are good flowability, spreadability and high packing density. The powder properties must allow for proper dosing of the feedstock from the hoppers, as well as spreading. They determine resulting powder layer characteristics, like the surface quality, packing fraction and homogeneity of the deposited layer along the building area. The desired bulk solid properties are fulfilled by the most frequently used and optimized commercial polymer feedstocks, namely PA12, PA11 and PA6, making up more that 90% of the market share. These PA powders with 40–90 microns primary particle size typically are produced either by direct polymerization (c.f. Orgasol, Arkema) or precipitation (Dechet et al., 2019), e.g. PA2200 (EOS) or DuraForm PA (3D Systems). Figure 4 depicts scanning electron microscopy (SEM) images of the commercial PA12 PBF-LB/P feedstock PA2200 (EOS). This material is characterized by 'potato-shaped', smooth particles being typical for particles produced by precipitation (see Figure 4A) (Schmid et al., 2015). Moreover, the PA12 powder shows a very narrow particle size distribution (PSD) characterized by a span ($(x_{10,3} - x_{90,3})/ x_{50,3}$) of 0.57 (with $x_{10,3}$ = 45.8 µm, $x_{50,3}$ = 61.4 µm, $x_{90,3}$ = 81.0 µm). Narrow PSD and the absence of fines is advantageous with respect to flowability and dense packing.

Plastic PBF powders are frequently surface-functionalized with flowing aids (c.f. Figure 4B) by dry coating. Metal powder feedstocks typically are produced by gas atomization from the melt or by wire arc approaches (Krinitcyn et al., 2021), thus, spherically shaped particles are obtained. Surface functionalization to tune flowability there is only necessary for cohesive materials of rather small primary particle size (<25 µm) (Karg et al., 2019). Furthermore, dry particle coating allows to tailor the absorptivity and energy input during the building job. Adhering nanoparticles enables also manipulation of the solidification, respectively, crystallization step with respect to the formed phase morphology and, thus, the properties of the manufactured device. In the following, we will first give an overview on methods applied for characterization of bulk solid properties of AM powders. Then, applications of dry particle coating in powder-based AM with respect to the aforementioned possibilities to improve process behavior and part characteristics are reviewed.

## 2 Characterization of bulk solid properties of PBF-AM feedstock materials

Many methods for bulk solid characterization of PBF-AM powders have been proposed so far. Although, it is a more or less open question, which approaches allow for characterization of the feedstocks at load and stress conditions that apply during powder delivery and powder spreading in PBF. The methods used to assess flow properties of AM powders can be subdivided into (quasi-)static and dynamic approaches being characterized by different consolidation states of the bulk solid prior to and strain rates during testing (Krantz et al., 2009; Ghadiri et al., 2020). Quasi-static approaches allow for characterization of bulk solid failure for flow initiation. An example for quasi-static testing are shear experiments e.g. in a ring shear cell, where

the failure of a confined, pre-consolidated powder to initiate flow can be determined as a function of applied load or consolidation time. Quasi-static methods give information on the agglomeration behavior, i.e., the cohesion of the bulk solid and, thus, are well suited to determine data necessary e.g. for the design of hoppers and silos. In contrast, dynamic approaches are applied, if flowability of a bulk solid needs to be determined under stress conditions that apply e.g. during fluidization or pneumatic conveying, where the bulk solid is non-consolidated and non-confined and the particles are in motion. Examples for dynamic testing methods are powder rheometers, where the resistance to shearing of an aerated, i.e. non-consolidated bulk solid is determined at different shearing speeds, or rotating drum testers, where the avalanching behavior of particles under motion at free-surface conditions is evaluated (Schwedes, 2003; Ghadiri et al., 2020). A frequently used approach to assess powder flowability of PBF-LB/P feedstocks, which is even proposed in the relevant norms, is the calculation of the Hausner ratio (HR), the ratio of the tapped density to the (loose) bulk density of the powder. Although giving information on the compaction behavior of a bulk solid, respectively, its cohesion, this quantity may be misleading, because notable changes in tapped density and bulk density are "eliminated" by calculation of the quotient of the two densities, as shown recently (Hesse et al., 2021). Moreover, HR is not very sensitive to subtle changes in bulk properties and completely unreliable, if the compaction is performed manually. The usage of tapped volumeters is mandatory if HR (or tapped density) shall be determined. Often, different flow characterization techniques yield contradicting results (Krantz et al., 2009; Chatham et al., 2019). Thus, for certain applications static and dynamic testing as well as powder spreading experiments, that account for the effect of jamming during powder deposition (Nan et al., 2018) are necessary for a comprehensive characterization of the bulk solid under different stress conditions. Also Leturia et al. (2014) pointed out, that a paramount description of powder flow behavior under different stress conditions cannot be achieved by a single index or a number, since flowability depends on intrinsic single particle properties (solid density, particle size, shape, roughness, Hamaker constant, tendency to adsorb water, work function to quantify particle charging) and bulk properties, i.e., the interaction of the single particles. Finally, external factors, such as temperature and humidity, but also the stresses acting on the bulk solid play a significant role. Two limiting states exist, the aerated bulk solid in a fluidized bed (unconfined, low stress level) and packed bed conditions (confined, high stress level) in a compacted powder. PBF feedstocks are subjected to rather low stress levels in the dynamic regime during powder application. The challenges to characterize powders under these conditions have been more recently addressed by Ghadiri et al. (2020). Especially in the case of polymer feedstocks it is essential to consider the effect of environmental conditions, first and foremost the process temperature in PBF, see for example Ruggi et al. (2020) and our own work (Hesse et al., 2021). In the following, selected approaches reported in the literature for bulk solid characterization of PBF feedstocks are outlined and their strengths and weaknesses with respect to feedstock material characterization under process conditions are discussed.

## 2.1 Flow meters

For characterization of PBF-LB/M and PBF-EB/M powders frequently flow meters are applied (Mellin et al., 2017; Pleass and Jothi, 2018; Cordova et al., 2019; Cordova et al., 2020), as these funnel tests were already employed as standard procedures for flowability characterization according to different standards for metal powder feedstocks used in other manufacturing processes (e.g. metal injection melting). Besides funnel flow tests, the determination of the angle of repose is recommended in norms to characterize metal AM feedstocks. For flow rate determination, first, a certain mass of the powder is filled into a funnel of defined geometry, with the funnel outlet closed. Subsequently, the orifice is opened and the time taken for the powder to flow out of the funnel is determined several times. As a final result the average of the flow rate is given. Faster flow is assigned to better powder flowability. The determined flow rate is a function of powder characteristics, such as PSD, shape, state of agglomeration or aggregation, surface characteristics (roughness, surface chemistry, presence and thickness of e.g. oxide layers), but it is also influenced by

i) the ambient conditions during measurement, i.e. temperature and relative humidity,
ii) pre-conditioning of the bulk solid to be characterized (c.f. e.g. drying, sieving, de-agglomeration, aeration),
iii) the funnel filling procedure, powder mass and,
iv) the funnel geometry (orifice diameter, angle), surface roughness and funnel material.

The Hall (Pleass and Jothi, 2018; Cordova et al., 2020), Gustavsson (Mellin et al., 2017) and Carney funnel (Larsson et al., 2016) have been applied for determination of the flow rate of metal PBF feedstocks. The funnels need to be made of metal and have a certain maximum surface roughness. Due to its larger orifice and steeper angle, the Carney funnel allows for measurement of flow rates of cohesive materials that cannot be determined with the Hall flow meter. Thus, the Carney funnel has been assessed as the preferred geometry for measurement of more cohesive powders (Pleass and Jothi, 2018). Contrary, the Gustavsson flow meter characterized by a small orifice was assessed to be superior, as it allowed for discrimination of the flowability of PBF feedstocks, that did not show different powder flow rates in the Hall flow meter (Mellin et al., 2017; Carrozza et al., 2020) . There is some general debate, if the procedure of

flow rate determination via these funnels experiments is sensitive enough to discriminate powders of e.g. different ageing state (Carrozza et al., 2020) and, thus, if the flow meters are an appropriate means for powder qualification and characterization of flowability and spreadability under PBF process conditions at all. Cordova et al. (2020) criticized that the determination of powder flowability with flow meters will not allow for proper characterization of metal PBF feedstocks, as it does not resemble the conditions (c.f. acting stresses) during powder spreading. Especially, the rather large funnel opening cannot mimick the effect of the rather small gap between powder bed and the wiper blade during powder spreading. We also assess the funnel flow tests as not sensitive enough to give information on a powder's behavior in the AM process. Although, the static angle of repose, which may be determined from the geometry of the powder heap (height, diameter) formed by a powder flowing out of a funnel has been shown to be a reasonable measure for flowability. However, its sensitivity, for example, was not sufficient to discriminate PA12 feedstocks of different ageing state (Hesse et al., 2021).

## 2.2 Shear testers

For measurement of flowability of powders in various applications, shear testers are applied (Jenike, 1964; Schwedes, 2003; Schulze, 2008). To this end, they have been used in characterization of PBF feedstocks as well (Blümel et al., 2015; Dechet et al., 2019; Ruggi et al., 2020). Measurement of flowability by direct shear testers and the classification of flow behavior by the flow function ffc was proposed by Jenike (Jenike, 1964). Various variants of shear testers including ring shear rotational testers like the Schulze cell (Schwedes, 2003) have been established. The original Jenike cell is made up of a (fixed) base, a ring and a lid. The inner surfaces of the cell are roughened to guarantee for good wall adhesion of the powder. After introducing powder and closing the lid, a normal force is applied to the lid and a shear force is applied to the cell. By doing shear experiments for identical pre-consolidated samples, the (maximum) shear stress $\tau_{max}$ is calculated as shear force divided by the cross-sectional area of the cell in dependence of the normal stress $\sigma$ (normal force divided by cross-sectional area), i.e., the yield locus ($\tau_{max}$ over $\sigma$) depending on the bulk density at a given pre-consolidation can be determined. From the yield locus, the unconfined yield stress, $\sigma_c$ and the consolidation stress $\sigma_1$ can be determined by the construction of Mohr's stress circles. Moreover, the internal angle of friction can be determined. For a detailed description of the measurement procedure, the construction of the yield locus and the determination of the aforementioned quantities, the reader is referred to e.g. a review by Schwedes (Schwedes, 2003) or a textbook by Schulze (Schulze, 2008).

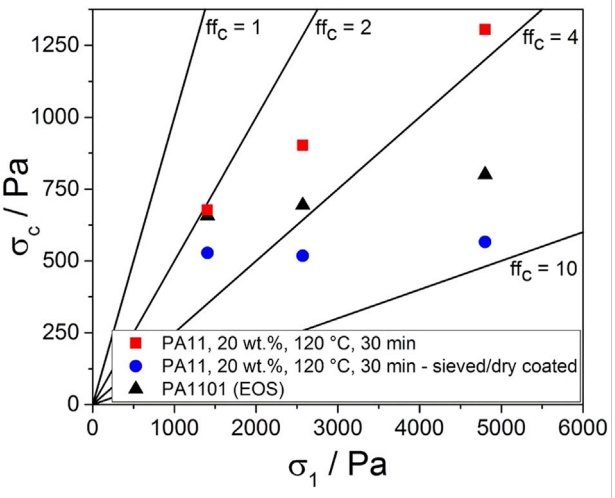


FIGURE 5
Unconfined yield strength $\sigma_c$ in dependence on consolidation stresses $\sigma_1$ of PA11 powders as determined from the yield locus measured by a ring shear tester. The flow function ffc = $\sigma_1$/ $\sigma_c$ allows to quantify flowability (reprinted from Dechet et al. (2019), Production of polyamide 11 microparticles for Additive Manufacturing by liquid-liquid phase separation and precipitation. Chemical Engineering Science 197, 11–25, Copyright (2019), with permission from Elsevier).

An example of shear experiments with different PA11 PBF feedstocks is given in Figure 5 depicting the flow functions ffc = $\sigma_1$/ $\sigma_c$, i.e., the ratio of the major consolidation stress $\sigma_1$ and the unconfined yield strength $\sigma_c$. The measurements were performed at ambient temperature and demonstrate how flowing aids and the removal of fines improve flowability. The red open squares in Figure 5 depict data of a PA11 powder obtained by precipitation of an injection molding grade Rilsan PA11 (Arkema) from ethanol at 120°C and 20-wt.% polymer concentration (Dechet et al., 2019). The as-obtained powder is characterized by a particle size of $x_{50,3}$ = 90 µm, a $x_{10,3}$ of 27 µm and a $x_{90,3}$ of 185 µm. The PSD is rather broad (span = 1.76). This material behaves cohesive (2 < ffc <4). For improvement of flowability, the PSD was narrowed by sieving and the sieved PA11 powder with $x_{10,3}$ = 34 µm, $x_{50,3}$ = 84 µm, $x_{90,3}$ = 165 µm (span = 1.56) was dry coated with 0.5 wt.-% of hydrophobic fumed silica (blue filled circles). The classified and functionalized powder is easy flowing (ffc >4) and –due to its larger size- shows superior flowability than a commercial PA11 feedstock (PA1101, EOS) of a mean particle size of 49 µm.

Although shear testing is a standard method for bulk solid characterization, it has not been applied frequently in characterization of PBF feedstocks (Lyckfeldt, 2013; Blümel et al., 2015; Schmidt et al., 2019b; Dechet et al., 2019; Ruggi et al., 2020; Dechet et al., 2021; Hesse et al., 2021) as compared to e.g. HR or funnel flow tests. This is surprising despite of the advantage, that shear testers allow for well-reproducible

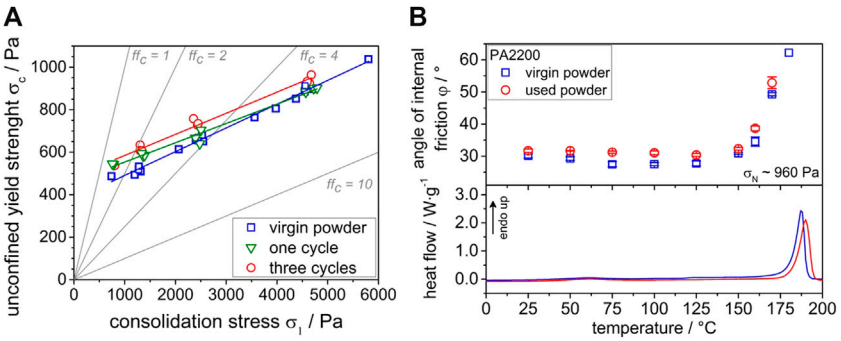


FIGURE 6
**(A)** Flow function for PA12 powders with varying aging states (one cycle implies 15.5 h of PBF-LB/P processing at 150°C building chamber temperature). **(B)** temperature-dependent angle of internal friction and thermograms for virgin and three times recycled PA12 powder (reprinted from Hesse et al. (2021), Towards a generally applicable methodology for the characterization of particle properties relevant to processing in powder bed fusion of polymers—From single particle to bulk solid behavior. Additive Manufacturing 41, 101,957, Copyright (2021), with permission from Elsevier).

measurements under defined load conditions and even at elevated temperature, which is especially important for polymer feedstocks (Ruggi et al., 2020; Hesse et al., 2021). As shown in Figure 5 shear experiments clearly allow to assess the effect of flowing aids on flowability. In (Blümel et al., 2015) a correlation of (large) ffc, (high) bulk density, (good) layer and single layer specimen quality was demonstrated for a PE powder used in PBF-LB/P, thus, shear testing allows optimization of powder properties during feedstock development. Moreover, a direct quantitative comparison of newly developed materials with established feedstocks via the flow function is straightforward. Correlations between the flow behavior quantified by ring shear experiments and device quality are well validated.

Criticism exists in using the obtained flow functions ffc for assessment of PBF processability, as ffc typically is determined at rather high consolidation stresses that do not apply during powder spreading (Spierings et al., 2016; Vock et al., 2019). Moreover, the flowability of a pre-consolidated bulk solid is determined under quasi-static conditions, which does not resemble the situation in powder spreading in PBF. For example, if a rake is used for powder deposition, typically a non-consolidated bulk solid is spread. Also if a roller is used, the bulk solid is applied as non-consolidated powder under dynamic conditions and the consolidation stress is rather low. Nonetheless, shear testing has been found to be a reliable and very sensitive method to compare powders that only show subtle differences. It is one of the rare approaches to assess feedstock behavior under process conditions, i.e. the building chamber temperature (Ruggi et al., 2020; Hesse et al., 2021). As shown in Figure 6, shear tests allow the monitoring of the deterioration of powder flowability upon ageing of PA12 feedstocks and, if performed in a heated cell, the flowability at building chamber temperature can be assessed (Figure 6B): the flowability at building chamber temperature of around 165–170°C is rather different from that at ambient temperatures. From around 150°C the PA12 powder behaves more and more cohesive, as seen from the increase of the angle of internal friction. The reason is most likely the onset of sintering, i.e. sintering necks largely enhance interparticle adhesion.

## 2.3 Rotating drum powder analyzer

The rotating disc (Kaye et al., 1995) or rotating drum powder analyzer is a device that allows to characterize the dynamic flow behavior of powders at free-surface conditions under motion (Schwedes, 2003). Testers based on this principle are available commercially e.g., as AeroFlow (TSI) or Revolution powder analyzer (Mercury Scientific). The acting stresses are typical for processes like e.g. blending, mixing or pneumatic conveying (Krantz et al., 2009) and, thus, this device has been judged as an appropriate method for mimicking the powder spreading process as well (Amado et al., 2011; Ziegelmeier et al., 2013; Ziegelmeier et al., 2015; Spierings et al., 2016). The working principle of the rotating drum powder analyzer is based on the characterization of the avalanche behavior (c.f. avalanche angle, avalanche frequency and mass) of the bulk solid, which is correlated with its flowability (Kaye et al., 1995; Schwedes, 2003). The drum is equipped with lateral glasses that allow for proper illumination and monitoring of its cross section by means of a camera. Upon rotation, the bulk solid is carried up the side of the drum until it collapses (around the (static) angle of repose) or fulfills an avalanching movement. The camera records binary images of the cross sectional area of the drum, which allows to determine the maximum avalanche angle, respectively, to calculate indices related to the flow behavior of the powder (Amado et al., 2011; Ziegelmeier et al., 2013; Spierings et al., 2016). A smaller avalanche angle corresponds to better

flowability. Amado et al. (Amado et al., 2011) claimed that setting the rotational speed to the translational speed of powder spreader allows to generate stresses that are a good approximation of that acting during spreading in PBF. Besides the avalanche angle, the evaluation of the surface fractal and the volume expansion ratio, respectively, have been proposed. The surface fractal is the fractal dimension of the free surface of the powder. It is a direct indication of the roughness of the powder surface and an indirect measure of the inter-particle forces (Amado et al., 2011; Spierings et al., 2016) and, thus, flowability under dynamic conditions. The volume expansion ratio is the ratio of the expanded volume of the powder in the drum during rotation and the tapped bulk volume of the powder in the sample preparation container. The expanded volume is determined by image processing as the portion of the area of the drum's cross section occupied by particles multiplied by the length of the drum.

## 2.4 Powder rheometers

In addition to shear characteristics under static load, powder rheometers allow the determination of flow characteristics (cohesion) under dynamic conditions, as well and quantification of bulk solid characteristics, such as density, compressibility or permeability under a wide variety of load conditions (from the fluidized to the compacted state) (Freeman, 2007; Clayton et al., 2015). The device consists of a volume chamber, which allows for fluidization of the bulk solid via a sinter metal base plate for conditioning, measurement and / or the determination of permeability. Moreover, it is equipped with a shaft that allows for driving probes of different geometry into the (fluidized) bulk solid and the determination and control of torque and rotational speed. The shaft is connected to a drive, respectively force transducer that allows for positioning in the vertical direction and normal force measurement and control. The sample is pre-conditioned in a "conditioning cycle" according to a standard protocol which allows to prepare a lightly packed powder sample (Freeman, 2007; Leturia et al., 2014). If the probe is a lid, the powder rheometer can be operated as a shear tester and the flow function can be determined. If the probe is a twisted blade, the powder rheometer allows for determination of various further empirical characteristics, amongst them the basic flowability energy (BFE) being the energy necessary for displacement of a powder during forced flow, the specific energy (SE) representing the bulk solid's resistance against displacement in an unconstrained environment, being e.g. sensitive on interlocking of particles, the stability index (SI) giving information on changing flow behavior when repeating the test protocol, and the flow rate index (FRI) giving information on the sensitivity of flow energy on the movement speed of the blade. BFE is determined via a blade traversing the pre-conditioned powder sample from the top to the bottom of the testing volume at constant blade speed (of 100 mm/s). The calculation of this 'displacement energy' is performed by considering the measured torque and normal force and the trajectory of the tip of the blade. SE is the displacement energy needed to move the rotating blade upwards through the pre-conditioned powder (at constant blade speed) normalized to the powder mass. The normalization to the powder mass allows for better comparability of samples, as it allows for compensation of bulk density. FRI gives the dependence of flow energy on blade velocity. It is determined by measuring the ratio of flow energies determined according to the procedure of BFE at a blade movement speed of 100 mm/s and 10 mm/s. After determination of BFE or SE, the adhesion of the tested bulk solid can be determined by an adhesion test, which simply is the determination of the amount of material adhering to the blade after removal. Moreover, the device allows measurement of fluidization curves. A more detailed description and the measurement protocol can be found in a paper by Freeman (Freeman, 2007).

Typically, multiple flow indicators determined with the blade method are used for assessment of the bulk solid's flow behavior. Measurements typical allow for a good comparison of similar materials, however, do not allow for discrimination of very different materials (Leturia et al., 2014). High BFE typically is found for more densely packed bulk solids of good flowability. Here, a higher energy is required to move the powder particles and force chains are established, as in contrast to cohesive materials showing small BFE (due to lower packing fraction) and high compressibility. With respect to metal PBF feedstocks, Clayton et al. (2015) demonstrated that the powder characteristics accessible by powder rheometry are sensitive on subtle differences of bulk solids of almost identical particle size distribution, that could not be resolved by angle of repose or Hall funnel measurements.

When comparing the methods allowing for characterization of bulk solid conditions at dynamic conditions at small loads and free surface conditions (cf. revolution drum analyzer, powder rheometer) with shear testing or methods relying on the determination of the compaction behavior, such as compressibility tests (Hesse et al., 2021), it was reported recently (Tan et al., 2021), that these flowability indicators correlate well with the avalanche angle (dynamic angle of repose) determined from powder spreading experiments. The authors investigated 12 materials under dynamic and static conditions as well as under compression and evaluated the correlation of the flowability descriptors by means of principal component analysis. The best correlation between avalanche angle from spreading experiments and these flowability descriptors was found for SE determined by a powder rheometer, although, for most materials there also were observed reasonable correlations (correlation coefficient >0.8) between the avalanche angle during spreading and quantities

deduced from shear or compression tests. Interestingly, a "dynamic" flowability descriptor, BFE showed a rather poor correlation with the observed avalanche angle.

# 3 Applications of dry particle coating for powder bed fusion additive manufacturing—An overview

In the following, an overview on the state of the art of dry particle coating of materials for application in additive manufacturing (AM) based on a literature survey conducted in May 2022 using the Scopus (Elsevier) database searching for the terms listed in the supporting information (Supplementary Table S1) in the categories title, abstract and keywords is given. The single search results have been combined and corrected for duplicate items. This resulted in a set of 182 individual items that have been reviewed by the authors and assessed, whether relevant or irrelevant for the addressed topic of dry coating in PBF of polymers and metals. Finally, a subset of 47 articles or conference papers related to (dry) particle coating and PBF of metals and a subset of 26 articles or conference papers related to (dry) particle coating and PBF of polymers were identified. These references, which are listed in the supporting information, have been complemented with further papers being relevant to the topic, which e.g. have been referred to in papers from the two aforementioned article subsets, but not found in the initial search and a selection of works being relevant to dry coating or powder bed fusion AM in general.

While dry particle coating of polymer feedstocks typically is used to improve flowability of feedstocks, in more recent papers attempts of nanoparticulate surface functionalization to tailor absorptivity or particle charge to tune their PBF processability have been reported. Moreover, nanoparticulate additives were applied to tune the crystallization behavior, respectively, to produce composite particle systems allowing for manufacture of functional electrically conductive or magnetic devices. The number of relevant papers related to coating of metal PBF exceeded the number of works related to polymer PBF. An improvement of the flowability of metal powder feedstocks often is not necessary, due to their more favorable particle shape (cf. almost perfect spherically shaped particles produced by gas atomization (Pazos et al., 2018)) and their lower (relative) cohesiveness in comparison to polymer particles, as expressed by the granular bond number, the ratio of vdW interaction force to the gravitational force (Schmidt et al., 2020; Gärtner et al., 2021). The functionalization of metal powders by nanoparticle (dry) coating was mainly motivated by the production of metal matrix composites and, thus, tuning the microstructure of the obtained part to improve mechanical part properties, such as e.g. hardness, tensile properties or elongation at break. Dry coating of metal AM powders for tuning the microstructure obviously attracted researchers' interest in recent years and is identified as a trending topic, as confirmed by 16 out of the 48 relevant items published in 2020, 20 in 2021 and 4 this year. Further motivation for dry particle coating of metal feedstocks was to tune their absorptivity and their behavior in AM upon illumination, respectively, improvements of part properties, a reduced tendency for cracking or improved thermal or electrical conductivity. Applications of dry particle coating of metal powders, respectively, the effect of additive enhancement with nanoparticles on AM processability and part properties is addressed for different alloys in Section 3.2. The applications of dry particle coating for functionalization of plastic feedstocks and the implications on processability will be addressed in the following section.

## 3.1 Dry particle coating of polymer feedstocks for powder bed fusion AM

The flowability of polymer PBF feedstocks typically needs to be improved to make them processable. However, only few systematic studies investigated the effect of dry particle coating and the chosen process conditions on the feedstock's behavior in PBF-AM and resulting part properties. The effect of flowing aids on the powder properties, their PBF processability and the part characteristics was investigated by Blümel (2015), Blümel et al. (2015) for a PE-HD (high density polyethylene) system. They used a tumbling mixer for dry coating of PE particles with 0.5 wt.-% fumed silica, which was either hydrophobic (T1) or hydrophilic (T2) at identical conditions. Figure 7 depicts the effect of the flowing aid on flowability, bulk density, AM process behavior (roughness of spread layer) and quality of single layer specimen. While the PE-HD composite powder obtained by dry coating with hydrophobic fumed silica T1 leads to an improvement of flowability, as reflected by a ffc in the range of 4–10 (easy flowing), dry coating with T2 does not improve flowability (ffc comparable to pristine PE-HD, cohesive). The bulk density of the PE-T2 composite powder is even worse than that of the pristine PE powder, while dry coating PE-HD with hydrophobic fumed silica was shown to increase bulk density remarkably. The effect of the surface functionalization of PE-HD (T1 vs. T2) on powder spreading and specimen properties is clearly seen in the AM process. While the composite system prepared from PE and hydrophilic silica shows poor spreadability leading to uneven powder layers with a lot of defects and, in consequence, to defective specimen, PE-HD powder dry coated with hydrophobic silica shows a good spreadability; homogeneous powder layers are formed and specimen of good quality are obtained.

The reason for this behavior is seen in the less homogeneous coating of (hydrophobic) PE-HD particles with hydrophilic fumed silica characterized by the presence of nanoparticle agglomerates on the polymer particle surfaces and, thus, a less efficient action of the flow enhancer to form a nano-rough

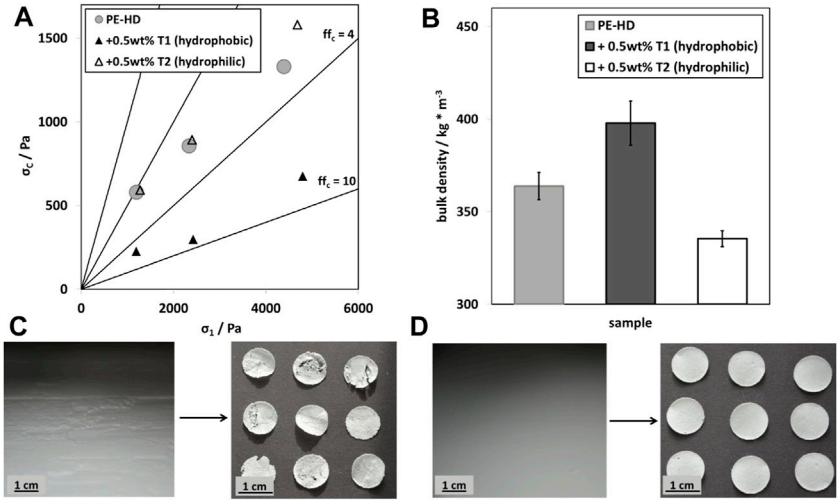


FIGURE 7
Effect of choice of flowing aid (hydrophobic silica T1 vs. hydrophilic silica T2) used to prepare PE-HD-silica composite powders on **(A)** flowability, **(B)** bulk density, spreadability (Figures 7**(C,D)** T1 vs. T2) under PBF process conditions and specimen characteristics (Blümel et al., 2015).

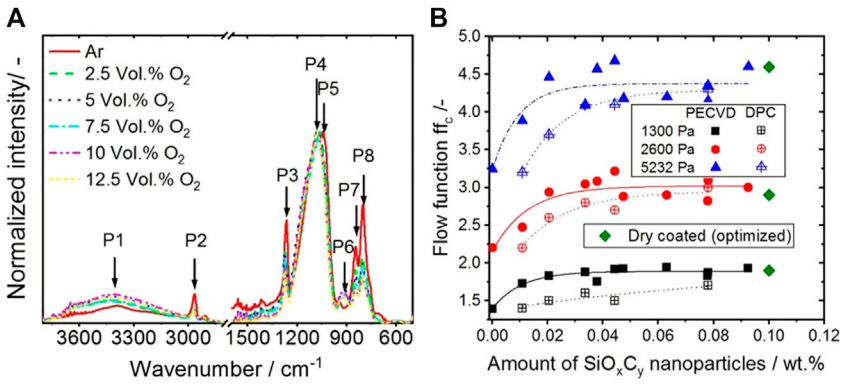


FIGURE 8
**(A)**: Tuning hydrophobicity of *in-situ* produced silica nanoparticles by choice of process gas composition (oxygen content) in PECVD functionalization of PP particles in a fluidized bed. **(B)** comparison of flowability of fluidized bed coated PP and PP particles obtained by dry particle coating (DPC) in a tumbling mixer in dependence on additive content: fluidized bed coating with *in-situ* produced silica nanoparticles allows for more improved coatings and, thus, lower additive content necessary to achieve a certain flow function ffc (reproduced from Gómez Bonilla et al. (2021a) under the CC BY-NC-ND 4.0 licence).

composite particle surface reducing particle interactions, as well as the water adsorption on hydrophilic silica nanoparticles allowing for formation of capillary bridges between asperities increasing the overall particle interactions. It is well-known that capillary bridges enhance the adhesion force between two particles by roughly one order of magnitude in comparison to vdW forces. The consequence of large particle-particle interaction forces is poor flowability and powder spreadability, often combined with low packing density.

Consequently, not only the choice of the type on nanoparticle coating material is important. Surface properties (Sachs et al., 2018) of nanoscale additives play a crucial role. This was demonstrated more recently by Gomez Bonilla et al. (2019), Gómez Bonilla et al. (2021a), who functionalized polypropylene (PP) powders in a fluidized bed reactor by *in-situ* produced silica nanoparticles of different surface termination via plasma-enhanced chemical vapor deposition (PECVD). They used an $Ar/O_2$ plasma jet for silica nanoparticle generation from a

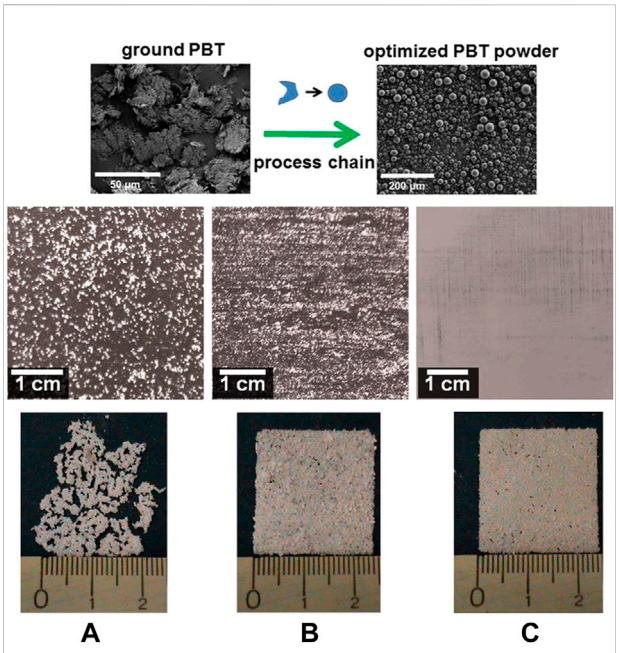


FIGURE 9
Effect of particle shape and surface functionality (ground PBT **(A)** vs. rounded PBT **(B)** vs. rounded and dry-coated PBT **(C)**) on powder spreadability and specimen quality (reprinted from Schmidt et al. (2016b)), Optimized polybutylene terephthalate powders for selective laser beam melting. Chemical Engineering Science 156, 1–10, Copyright (2016), with permission from Elsevier).

hexamethyldisiloxane precursor. The plasma nozzle was installed in the center of the distributor plate of the fluidized bed reactor and the choice of composition of the plasma gas ($O_2$ content) allowed for *in-situ* production of nanoparticles $SiO_xC_y$ of different hydrophobicity as confirmed by FTIR spectroscopy (Figure 8A). At 12.5 vol.-% $O_2$ nanoparticles close to the composition $SiO_2$ are formed, whereas in the Ar plasma without $O_2$ addition particles of the composition $SiO_{1.52}C_{2.3}$ were obtained. The authors compared the plasma-enhanced fluidized bed coating with dry particle coating and improved this way the flowability considerably, as measured by shear tests. Silica nanoparticle concentrations as low as 0.02 wt.-% for the fluidized bed coating were sufficient whereas dry particle coating (DPC) in a tumbling mixer required 0.1 wt.-% as optimum additive concentration for a comparable flowability increase (Figure 8B). This is explained by a much better dispersion of the nanoparticles by the direct synthesis in contrast to the tumbling mixer with only moderate dispersion of agglomerates. The amount of flowing aid in an AM feedstock powder should be kept as low as possible, as it might impair the isothermal crystallization behavior under process conditions (Tischer et al., 2022), i.e. lead to unwanted effects during processing, such as premature crystallization and, thus, deterioration of part geometry or termination of the built. Moreover, a too high flowing aid content was shown to impair the melt coalescence necessary to assure dense parts and good layer adhesion. All these interconnected effects along the whole process chain influence the final mechanical and functional properties of the produced parts (Kleijnen et al., 2019).

The effect of particle shape and surface functionalization on particle interactions, powder spreadability and quality of L-PBF-produced specimen were investigated by Schmidt et al. for a process chain consisting of (wet) comminution of polymers (Schmidt et al., 2012), thermal rounding in a heated downer reactor (Sachs et al., 2017; Gómez Bonilla et al., 2021b) and dry particle coating in a tumbling mixer for polystyrene (PS) (Schmidt et al., 2014; Schmidt et al., 2015), polybutylene terephthalate (PBT) (Schmidt et al., 2016a; Schmidt et al., 2016b; Schmidt et al., 2016c) and composite powder systems (filled systems, e.g. PBT-glass, PBT-$Al_2O_3$ and blends, e.g. PBT-polycarbonate (PC)) (Dechet et al., 2018; Schmidt et al., 2019a). These examples show, that this process chain approach is applicable to any thermoplast that shows grindability, including systems that attracted interest recently, like bio polymers or high temperature thermoplasts.

The effect of particle properties along the powder production process chain and the effect of particle properties (shape, particle interactions) on powder spreadability and specimen characteristics is exemplarily depicted for PBT (Schmidt et al., 2016b) in Figure 9. In a first step, cold wet comminution in ethanol in stirred media mills at reduced temperatures was used to produce PBT particles of around 20 µm size ($x_{50,3}$). The obtained product (see Figure 9, left) consisted of angular and plate-like particles that were cohesive (powder tensile strength (Zimmermann et al., 2004; Schmidt et al., 2019b): (15.7 ± 0.8) Pa), had a low bulk density (0.25 g/cm$^3$) and showed poor powder spreadability, as quantified by image analysis ((19.1 ± 4.2) % surface coverage). Thermal rounding of the comminution product in the heated downer reactor allows for production of almost perfectly spherical particles. These powders show an improved flowability (powder tensile strength (10.7 ± 1.7) Pa) and bulk density (0.47 g/cm$^3$)). The spreadability is also improved for the rounded product. After dry particle coating (with 0.5 wt.-% fumed silica), almost complete coverage of the substrate ((97.3 ± 1.8) %) and, thus, good spreadability and excellent flowability (powder tensile strength: (2.9±0.6) Pa) were achieved. From the rounded and dry coated powder dense specimen could be successfully produced, while this was not possible from the wet ground, angular and cohesive particles. The specimen produced from the dry particle coated composite material showed a lower surface roughness than specimen produced from non-coated, rounded material. An improvement of AM processability upon dry coating was also found for melt-emulsified, narrowly-distributed spherical PP powders (Fanselow et al., 2016; Schmidt et al., 2017), i.e. even for ideally shaped particle systems dry coating improves AM

TABLE 1 Overview on applications of (dry) particle coating reported in the literature to tune polymer AM feedstock's processability, respectively, resulting component properties.

| Host particle material | Guest nano-particles | Coating device / method | Tuned powder property | Processability / part properties | References |
|---|---|---|---|---|---|
| PE-HD | $SiO_2$ hydrophobic vs. hydrophilic (Aerosil, Evonik) | Tumbling mixer | Flowability, packing density, spreadability | Improved spreadability and dense specimen for PE-$SiO_2$ (hydrophilic) | Blümel, (2015), Blümel et al. (2015) |
| PP | $SiO_2$ of tunable surface termination, *in-situ* produced via PECVD | Fluidized bed | Flowability, packing density, spreadability | N/A | Gomez Bonilla et al. (2019), Gómez Bonilla et al. (2021a) |
| PS / PBT / PBT-PC / PBT-glass / PBT-$Al_2O_3$/ PP / PC / PA11 | $SiO_2$ (Aerosil, Evonik) | Tumbling mixer | Flowability, packing density, spreadability | Improved spreadability and dense specimen | Schmidt et al. (2014), Schmidt et al. (2015), Schmidt et al. (2016a), Schmidt et al. (2016b), Schmidt et al. (2017), Dechet et al. (2018), Kloos et al. (2018), Dechet et al. (2019), Schmidt et al. (2019a), Dechet et al. (2021) |
| PE | Carbon black (CB) | Tumbling mixer | Flowability, absorption, conductivity | Improved spreadability and absorption, electrically conductive specimen | Blümel et al. (2014) |
| PA12 | CB | Planetary mill | Flowability, absorption, tribo charging | Improved spreadability and absorption, parts of higher strength | Xi et al. (2020) |
| PP | Fumed $SiO_2$ (Aerosil, Evonik) | Mixer | Flowability, particle charge | Improved spreadability, more dense parts of higher tensile strength and Young's modulus | Lexow and Drummer, (2016) |
| PP | Fumed $SiO_2$, (HDK H05TX (negatively charging) and HDK H05TA 3 (positively charging), Wacker Chemie) | Tumbling mixer | Flowability, charge control | Improved spreadability, photoelectric powder deposition | Düsenberg et al. (2022a), Düsenberg et al. (2022b) |
| PA12 | Iron oxide, C, Ag, *in-situ* produced by laser fragmentation in liquid | Wet coating from dispersion | Absorption, magnetism | Absorption, production of magnetic devices (iron oxide), tuned microstructure / spherulites (C, Ag) | Hupfeld et al. (2020a), Hupfeld et al. (2020b), Hupfeld et al. (2020c), Hupfeld et al. (2020d), Sommereyns et al. (2021b), Sommereyns et al. (2021a) |
| PA12 / PEEK | Carbon nanoplatelets, graphene, fullerene-type $WS_2$ | Wet coating from dispersion | Flowability, absorption | Improved mechanical part properties | Yazdani et al. (2018), Chen et al. (2020) |

processability. This has been also confirmed for precipitated "potato-shaped" powders (Kloos et al., 2018; Dechet et al., 2019; Dechet et al., 2021) like shown in Figure 4 in shear tests depicted for PA11 in Figure 5.

Dry particle coating of AM feedstocks may not only be used to tune flowability; it may be also applied to tailor absorptivity of polymer powders, respectively, to tune electrical, magnetic and charge properties. Applications, that will be addressed in the following, are summarized in Table 1. Blümel et al. (2014) applied carbon black (CB) nanoparticles to PE by dry coating in a turbular mixer. The obtained composite powder could be processed at reduced laser energy input and the parts showed electrical conductivity above the percolation threshold. More recently, Xi et al. (2020) dry coated cryogenically ground PA12 with CB in a planetary ball mill. Parts produced from the PA12-CB powder showed improved mechanical properties, which has been ascribed to the action of CB as a flowing agent, but also to enhanced electrical conductivity and, thus, minimizing implications of tribo charging.

TABLE 2 Overview on (dry) coating of metal AM feedstocks for tailoring powder properties, respectively, processability and component properties.

| Host particle system | Guest nanoparticles | Coating device / method | Tuned powder property | Processability / Part properties | References |
|---|---|---|---|---|---|
| Steel (1.4404, 1.2709) | SiC, iron oxide, few layer graphene | Fluidized bed | Flowability, absorption | Improved spreadability and laser absorption, more dense MMC parts of improved mechanical properties, hardness, wear resistance | Lüddecke et al. (2021), Pannitz et al. (2021) |
| Steel (1.4404) | $Y_2O_3$ | High energy mill, wet coating from dispersion | Flowability | Parts of improved mechanical properties and hardness due to grain refinement and dispersion strengthening | Doñate-Buendia et al. (2020), Zhai et al. (2020) |
| Steel (1.4404) | $SiO_2$ | Tumbling mixer | Flowability, packing fraction | Increase powder bed and green body density of parts produced by binder jetting | Shad et al. (2021) |
| Al-Si / Al-Cu | $SiO_2$ | Tumbling mixer | Flowability | Increased part density | Karg et al. (2018), Karg et al. (2019) |
| Various Al alloys | AlN, SiC, TiC, $TiB_2$, TiN, $CaB_6$, $LaB_6$ | Shaker mixer, ball mill, planetary mill | Flowability, absorption | Improved absorption and process stability, parts of improved mechanical properties, reduction of hot cracks due to grain refinement, respectively, columnar-to-equiaxed grain transition, dispersion strengthening | Kusoglu et al. (2020), Tan et al. (2020), Vieth et al. (2020), Wang and Shi, (2020), Xinwei et al. (2020), Heiland et al. (2021), Li et al. (2021), Mair et al. (2021), Sun et al. (2021), Wu et al. (2021), Zhuravlev et al. (2021), Mair et al. (2022), Minasyan and Hussainova, (2022), Qu et al. (2022) |
| Nickel alloys | TiC, $Al_2O_3$, $Y_2O_3$, | High speed mixer, tumbling mixer, planetary mill, wet coating from dispersion | Absorption | Improved hardness, tensile strength, elongation at break, reduction of hot cracks due to grain refinement, respectively, columnar-to-equiaxed grain transition, dispersion strengthening | Sehrt et al. (2017), Yao et al. (2017), Han et al. (2019), Guo et al. (2020), Han et al. (2020), Zhou et al. (2020c) |
| Cu / CuCr0.3 / CuCr1 | Carbon black | Tumbling mixer | Absorption | Improved absorption, reducing agent, improved mechanical and electrical part properties | Jadhav et al. (2019), Jadhav et al. (2020), Jadhav et al. (2021) |
| CuCr0.8 | TiC | Ball mill | Absorption | Improved absorption, improved mechanical properties | Shen et al. (2022) |
| Cu | CuS, $TiB_2$, multilayer graphene | Drop casting | Absorption | Improved absorption, improved mechanical properties | Tertuliano et al. (2022) |
| W | ZrC | High energy mill | N/A | Increased density of parts, improved mechanical properties due to grain refinement / suppression of columnar grain growth | Li et al. (2019) |
| TiAl6V4 | SiC | Ball mill | N/A | improved micro hardness, impact strength and less wear due to grain refinement and dispersion strengthening | Zhang et al. (2019) |
| AZ91D (Mg alloy) | SiC | Ball mill | N/A | improved mechanical properties due to grain refinement | Niu et al. (2021) |
| Zn | CNT@Ag | High energy mill | N/A | | Shuai et al. (2021) |

(Continued on following page)

TABLE 2 (*Continued*) Overview on (dry) coating of metal AM feedstocks for tailoring powder properties, respectively, processability and component properties.

| Host particle system | Guest nanoparticles | Coating device / method | Tuned powder property | Processability / Part properties | References |
|---|---|---|---|---|---|
| | | | | Improved mechanical properties (strength, ductility) due to CNT reinforcement | |
| AMZ4 (Zr-based bulk metallic glass) | $SiO_2$ | Tumbling mixer | Flowability | Improved spreadability | Wegner et al. (2021) |
| MoTiAl | $Al_2O_3$ + CNT | Hetero aggregation in liquid phase | N/A | Improved corrosion resistance due to formation of a ceramic layer at the part surface during PBF | Zhou et al. (2018), Zhou et al. (2020a), Zhou et al. (2020b) |

Moreover, also Xi et al. reported the effect of increased laser absorption allowing for manufacture at lower energy input. The effect of flowing aids applied as antistatics was also reported by Lexow and Drummer (Lexow and Drummer, 2016), while Düsenberg at al. (Düsenberg et al., 2022a; Düsenberg et al., 2022b). demonstrated that the tribo charging behavior of PP can be tuned by dry coating with fumed oxides: coating with HDK H05TX (Wacker Chemie), which exhibits HMDS/PDMS surface-termination, allows to produce a negatively charging composite powder, while coating PP with HDK H05TA 3 (Wacker Chemie), which exhibits PDMS / amine (-$NR_2$) termination, yields positively charging feedstock. Functionalization with these charging additives did not alter the melt crystallization behavior significantly. Defined charging of polymer powders is important for alternative AM powder deposition approaches via principles derived from electrophotography. Besides charge control, dry coating with these nanoparticulate additives also improved flowability. Dry coating also was investigated for laser direct structuring (Gath and Drummer, 2016) for formation of circuit board tracks on PBT components.

Besides dry coating, wet coating from dispersion was investigated as an approach towards composite feedstocks. AM-built magnetic parts could be produced from PA12 (wet) coated with iron oxide nanoparticles (Hupfeld et al., 2020b). Moreover, an improvement of mechanical properties in parts produced from composite powders of PA12-carbon nanoplateletes or from PEEK (wet) coated with fullerene-like $WS_2$ and graphene nanoplatelets was reported (Yazdani et al., 2018; Chen et al., 2020). Hupfeld et al. (2020c), Hupfeld et al. (2020d) demonstrated that the crystallization behavior of PA12 feedstocks and their microstructure (spherulites, lamellae) can be tuned by (wet) coating with carbon nanoparticles, respectively, Ag nanoparticles produced *in-situ* in the liquid phase by laser-induced fragmentation of precursors (Hupfeld et al., 2020a; Sommereyns et al., 2021a; Sommereyns et al., 2021b). These authors observed improved homogeneity of the nanoparticulate coating, if the functionalization was performed by wet coating from dispersion as compared to dry particle coating. Thus, smaller amounts of additives were necessary. Their observations are in good agreement with the report of Gómez Bonilla et al. (2021a) on dry particle coating in a fluidized bed with *in-situ* produced nanoparticles due to the excellent dispersed state of these nanomaterials.

## 3.2 Dry coating of metal feedstocks for PBF-AM

Within this section, applications of dry particle coating of metal AM feedstocks will be reviewed for the most frequently used feedstock materials, namely steel, aluminum, nickel and copper alloys. Applications of dry particle coating for further metal AM systems are summarized in Section 3.2.5. A tabular summary of the applications of dry coating to tailor metal PBF feedstocks, processability and part properties is given in Table 2.

### 3.2.1 Steel powders

Steel powders are interesting for L-PBF for the direct manufacture of functional tools with complex geometries and appropriate mechanical properties. Dry particle coating of steel and tool steel powder feedstocks improves PBF-LB/M processability and the resulting part properties via increasing flowability and enhancing laser absorption (Lüddecke et al., 2021; Pannitz et al., 2021). It is also an interesting, simple option for the production of metal matrix composite (MMC) powders (Zhou et al., 2020b) for manufacture of oxide dispersion strengthened (ODS) steel parts (Zhai et al., 2020) as compared to reactive synthesis during gas atomization or within the AM process (Pazos et al., 2018; Paul et al., 2020). ODS steel parts show high creep resistance and improved mechanical properties at high temperatures (Doñate-Buendia et al., 2021).

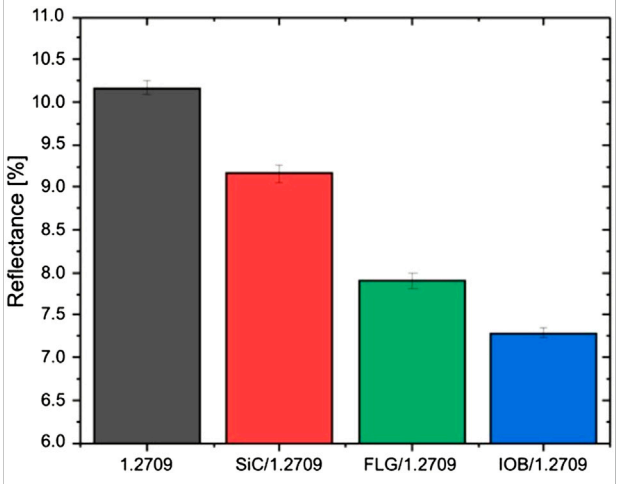


FIGURE 10
Reflectance measurements of coated and uncoated tool steel 1.2709 powder at a wavenumber of 9398 $cm^{-1}$. (reproduced from Pannitz et al. (2021) under the CC BY 4.0 licence).

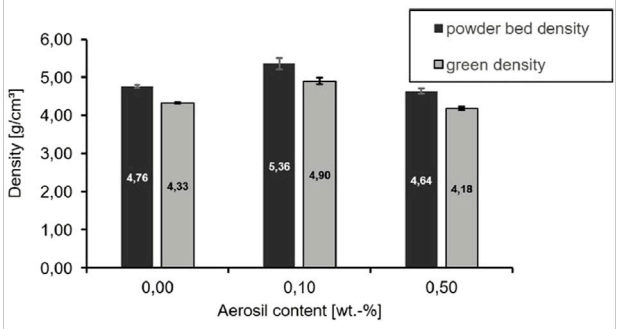


FIGURE 11
Results for powder bed density and green density of 1.4404 powder ($x_{50,3}$ =12.6 µm) with different amounts of fumed silica (reproduced from Shad et al. (2021), without any changes under the CC BY-NC-ND 4.0 licence).

Surface functionalization of steel with SiC is known to improve tensile strength as well as hardness and wear properties. Lüddecke et al. (2021) dry coated stainless steel (1.4404) and tool steel (1.2709) microparticles of 41 and 32 µm particle size ($x_{50,3}$) with SiC, iron oxide nanoparticles (IOB) and few layer graphene (FLG) in a fluidized bed. The nanomaterials were obtained by stirred media milling and used at guest particle concentrations between 0.2 wt%/vol% and 1.2 wt %/vol% with respect to the host powder. The authors studied the effect of surface functionalization on laser absorption and bulk solid properties of the obtained MMC powders by absorption and reflectance spectroscopy, bulk density determination, shear experiments, determination of the avalanche angle in a rotating drum setup, respectively, the cohesion strength and permeability by means of a powder rheometer. A good correlation between the aforementioned bulk solid characterization approaches was found. Tool steel (1.2709) powders functionalized with FLG (Pannitz et al., 2021) allowed for manufacture of dense parts (99.9% relative density) at an increased built rate and at lower laser energy as compared to the non-functionalized feedstock due to the decreased reflectance (see reflectance measurements depicted in Figure 10) of the composite powder and, thus, the higher energy input. Moreover, increased hardness values of the as-built parts were observed.

Also $Y_2O_3$ could be employed for preparation of stainless steel (1.4404) MMC powders by particle coating in a tumbling mixer, respectively, by high energy milling (Zhai et al., 2020). The obtained composite powders with $Y_2O_3$ concentrations between 0.3 wt.-% and 1 wt.-% could be processed via PBF-LB/M. Parts of acceptable relative densities between 99.2 % and 99.6% were obtained. Although, agglomeration of the $Y_2O_3$ nanoparticles and an increase in porosity with increasing $Y_2O_3$ concentration was observed. Doñate-Buendia et al. (2020), Doñate-Buendia et al. (2021) also addressed Yttria-nanoparticle coated steel powders for application in PBF-LB/M and directed energy deposition (DED-LB/M). They coated the host particles from suspensions of $Y_2O_3$ nanoparticles produced *in situ* by laser fragmentation in liquids and obtained steel powders surface functionalized with $Y_2O_3$ at a concentration of 0.08 wt.-%. The materials were processed by PBF-LB/M and the microstructure of the obtained ODS parts was studied in detail. The resulting distribution of nanoparticles in the metal matrix was assessed experimentally as well as by simulations (Yang et al., 2021). Homogeneous distribution of the Yttria nanoparticles within the matrix and a smaller grain size as compared to the parts manufactured from powders without $Y_2O_3$ addition were observed. The improved microstructure led to an increase in hardness by 9% and an increase of the compressive strength at 600°C of 29%.

Shad et al. (2021) investigated the effect of dry particle coating of different 1.4404 steel powders in the size range ($x_{50,3}$) of 4.4 and 12.6 µm with fumed silica at guest particle concentrations up to 1 wt.-% in a turbular shaker. The composite powders were prepared for application in binder jetting to prepare steel green bodies. An increase in the bulk and the tapped density of the coated powders of up to 40% and 11% as compared to the feed steel materials was observed at optimum silica content of around 0.1 wt.-%. Processing the optimized feedstock powders leads to an increase in the density of the green body (cf. Figure 11) and, thus, improved part properties.

### 3.2.2 Aluminum alloy feedstock powders

A known issue in processing aluminum alloys in PBF-LB/M is the formation of hot cracks within the built parts due to columnar grain growth as a consequence of the high thermal gradient during the built. Accordingly, the components

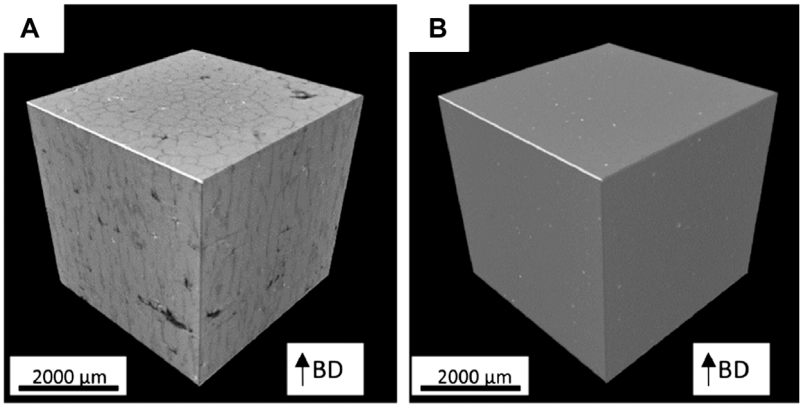


FIGURE 12
X-ray microscopy (XRM) images of **(A)** a specimen built from non-functionalized Al 2024; and **(B)** a specimen built from Al2024 powder dry coated with $CaB_6$ nanoparticles by PBF-LB/M (specimens in as-built condition). Reproduced from Mair et al. (2021) under the CC BY 4.0 licence).

mechanical strength decreases and undesired anisotropic mechanical part properties are obtained (Tan et al., 2020). A promising approach to obtain crack-free parts is grain refinement by addition of nanoparticles, such as carbides, nitrides or borides (see Table 2) to aluminum alloys (Kusoglu et al., 2020; Sun et al., 2021; Minasyan and Hussainova, 2022).

Heiland et al. (2021) dry coated Al7075 with 2.5 wt% TiC nanoparticles in a ball mill and successfully produced crack-free parts by PBF-LB/M due to the action of TiC as a nucleating agent. TiC lead to a refined microstructure and suppressed columnar grain growth (Zhuravlev et al., 2021). An analogous behavior was reported for Al-Si-Mg-Ti powder dry coated with TiC (Xinwei et al., 2020). Also wet coating of Al7075 (Vieth et al., 2020) and AlSi10Mg (Wang and Shi, 2020) with TiC nanoparticles by means of ultrasonication and wet ball milling was shown to be a feasible functionalization approach, although this process route has the drawback to demand for an additional drying step and potential contamination or oxidation of the alloy. Also for parts manufactured from Al6061/TiC composite powder prepared by planetary ball milling, a reduction of cracks was observed (Qu et al., 2022). Moreover, the authors observed improved PBF-LB/M processability characterized by a more stable process and the elimination of large spatters, which may lead to defective parts, for the composite powder system. This was ascribed to changes in the melt pool stability, respectively, droplet coalescence dynamics induced by the nanoparticles.

TiN was demonstrated to be an effective grain refiner for Al alloys as well, leading to additively manufactured parts with enhanced mechanical properties (Li et al., 2021; Wu et al., 2021). Wu et al. (2021) prepared Al7075/TiN composite powder with uniformly dispersed guest particles by a two-stage dry coating process consisting of ultrasonic –pre-mixing for 80 min of host and guest particles and subsequent coating in a V-type mixer for 12 h. The composite powder showed increased laser absorptivity due to the presence of TiN leading to a more favorable melt pool temperature profile. At a TiN content of 2 wt.-% crack formation could be eliminated completely due to formation of equiaxed grains. The grain refinement leads to parts of superior strength and improved micro hardness.

Mair et al. (2021), Mair et al. (2022) dry coated Al2024 particles with $CaB_6$ nanoparticles via planetary ball milling and observed an improvement of AM processability of the composite powder system. The composite powder showed lower reflectivity and higher bulk density than the Al2024 feedstock. $CaB_6$ nanoparticles induced a columnar to equiaxed transition of the microstructure in the built parts, leading to crack-free and pore-free, dense specimen without preferred grain orientation, high strength, elongation at break and hardness. The authors applied X-ray microscopy to quantify porosity and cracks within the built specimen as depicted in Figure 12. Grain refinement during PBF-LB/M of AlSi10Mg coated with 0.5 wt% $LaB_6$ nanoparticles using a shaker mixer was observed by Tan et al. (2020). The authors succeeded in the manufacture of isotropic, homogenous, crack-free parts that were characterized by an equiaxed and very fine-grained microstructure.

Dry coating also was exploited to tune flowability of very fine (<20 µm), cohesive Al powders. Karg et al. (2018) dry coated Al-Si with 0.5 wt% fumed silica and obtained a composite powder of improved flowability showing more homogeneous powder spreading, which allowed for manufacture of denser parts compared to the non-coated feedstock. The authors assessed the flow behavior by determination of the (static) angle of repose. Analogous observations were reported for Al-Cu mixtures dry coated with fumed silica (Karg et al., 2019).

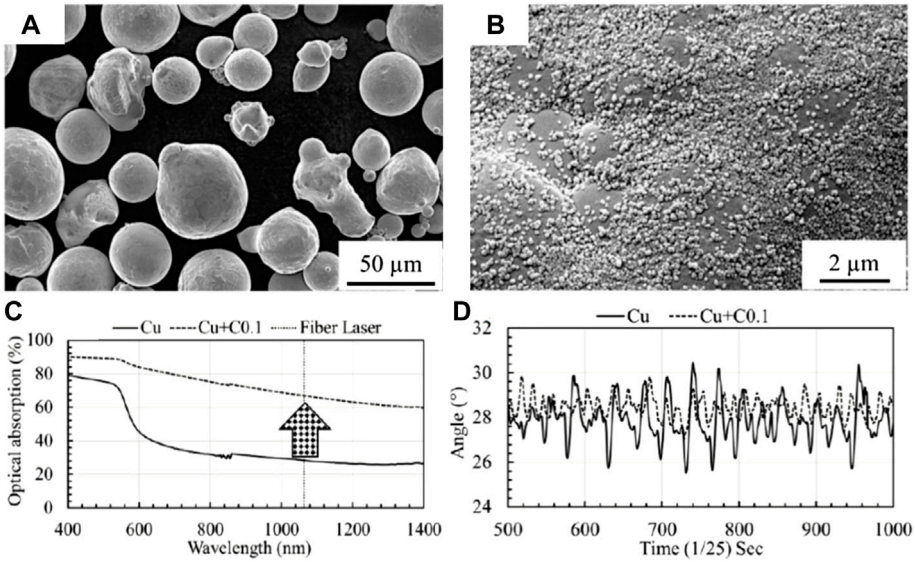


FIGURE 13
**(A)** SEM images of as-received copper particles, **(B)** surface detail of a Cu particle dry coated with carbon nanoparticles, **(C)** absorption of pure copper and 0.1 wt% carbon-mixed-copper and **(D)** temporal evolution of the avalanche angle observed for these powder systems. Reproduced from Jadhav et al. (2019) under the CC BY 4.0 licence).

### 3.2.3 Nickel alloy feedstock powders

Nickel alloys, especially super-alloys such as Hastelloy, are interesting for manufacture of corrosion-resistant turbine components exhibiting good mechanical performance at very high temperatures. AM of Ni super-alloys is challenging, because they are known to be susceptible to hot cracking due to anisotropic grain growth (Han et al., 2019). For modification of the resulting microstructure of the AM-built component, nanoparticulate grain refiners can be employed as well.

Han et al. (2019); Han et al. (2020) prepared surface-functionalized Hastelloy X powder with 1 wt% of TiC nanoparticles in a high speed mixer and investigated the effect of TiC on AM processibility, resulting microstructure and mechanical part properties. They confirmed that TiC functionalization induced formation of increased low angle grain boundaries leading to crack-free parts with tensile strength and elongation at break increased by 10 % and 19%, respectively. An improvement of mechanical properties by functionalization of Hastelloy X also was found by Sehrt et al. (2017). They adsorbed $Al_2O_3$ nanoparticles onto Hastelloy X from ethanol. The components produced from the composite powder showed improved micro hardness, although an increased part porosity due to $Al_2O_3$ agglomerates present was observed.

Zhou et al. (2020c) demonstrated that non-weldable Inconel 738LC could be processed to crack-free parts, if a composite feedstock containing 2.5 wt% TiC nanoparticles was used. Inconel host particles were coated with TiC in a planetary ball mill. Grains with a decreased aspect ratio were observed in parts manufactured from the composite. Moreover, TiC inhibited micro-crack formation. Parts showed a remarkable improvement in mechanical properties (ultimate tensile strength: (633 ± 34) MPa vs. (1,207 ± 4) MPa, elongation at break: (1.3 ± 0.3) % vs. (5.7 ± 0.2) %) as compared to specimen produced from the non-functionalized feedstock. Yao et al. (2017), reported the manufacture of near fully dense TiC matrix-reinforced Inconel 718 parts characterized by a refined microstructure from a composite powder produced by dry coating of gas atomized IN718 with TiC nanoparticles using a tumbling mixer. Specimens built from the composite powder showed an improved tensile strength due the grain refinement.

Guo et al. (2020) decorated INC738LC with Yttria nanoparticles by means of dry coating in a turbular mixer and studied the corrosion resistance of PBF-LB/M-produced parts at 1,095°C. $Y_2O_3$ addition of 0.05 wt% was found to increase corrosion resistance of the obtained components, although a grain coarsening was observed. They argued that the unexpected grain coarsening was due to formation of $Y_4Al_2O_9$ particles of low thermal conductivity. These particles led to a reduced cooling rate during the built leading to coarser grains within the component. Kenel et al. (2021) functionalized gas-atomized Ni-8Cr-5.5Al-1Ti powders with 0.5 wt.-% $Y_2O_3$ nanoparticles by ball milling and used the obtained composite powder in PBF-LB/M. Although $Y_2O_3$ nanoparticles could be successfully introduced into the matrix, they observed a lower alloy density due to nanoparticle incorporation and undesired

reactions with the alloy components. For instance, the formation of $Y_4Al_2O_9$ slag was observed preventing consolidation of the alloy or the formation of a $Ni_{17}Y_2$ phase promoting cracking.

### 3.2.4 Copper alloy feedstock powders

Additive manufacturing of copper components is especially interesting for applications where the large heat conductivity of the material is combined with complex shapes, like in AM-built heat exchangers. Moreover, copper can be used for AM-built parts of excellent electrical conductivity. Copper and its alloys are characterized by a large reflectivity (Jadhav et al., 2019; Jadhav et al., 2020; Jadhav et al., 2021), which makes them difficult to process, thus, it is necessary to apply rather large laser power.

In consequence, Jadhav et al. (2019) investigated the effect of surface functionalization of copper feedstocks with carbon black (CB) nanoparticles by means of dry coating on their absorption, flowability, PBF processability and resulting part properties. Dry particle coating of gas-atomized Cu powder with 0.1 wt% CB was performed under Ar atmosphere for 12 h in a Turbula mixer. The obtained composite powder was characterized by a homogeneous coverage of the mostly spherically shaped Cu host microparticles with CB nanoparticles (Figure 13). Bulk solid as well as optical properties of the Cu feedstock and the composite powder were characterized by determination of the avalanche angle and reflectance spectroscopy, respectively. The composite powder showed a higher absorptivity (67%) as compared to the non-functionalized feedstock (absorptivity: 29%) at the wavelength of the used fiber laser (1,080 nm). Moreover, it was characterized by an increased flowability expressed by a smaller dynamic angle of repose as compared to the feed material. Dense parts could be produced from the composite feedstock at lower laser energies, although the mechanical part properties were rather weak due to oxidation and phosphorous impurities along grain boundaries. The same authors transferred their approach to CuCr1 and CuCr0.3 alloys (Jadhav et al., 2020; Jadhav et al., 2021). Besides improvement of absorption by CB functionalization they noted that these nanoparticles also allow for reduction of oxide impurities during the PBF-LB/M process. Dense parts of improved strength and high conductivity could be produced.

Also Shen et al. (2022) applied surface functionalization of a Cu alloy to tune its absorptivity at 1,064 nm. They used a ball mill for dry coating CuCr0.8 with TiC. The laser absorption of the functionalized feedstock was 60% as compared to 30.5% for the non-functionalized one. Dense specimen of improved mechanical properties could be produced from the composite feedstock.

Tertuliano et al. (2022) investigated the functionalization of Cu powders with CuS, $TiB_2$, multilayer graphene flakes by drop casting to tune absorptivity. The aforementioned nanomaterials enhanced absorptivity of the composite powder and improved processability. The graphene functionalization was most efficient for the manufacture of dense specimen at reduced energy input as compared to the pristine Cu feedstock.

### 3.2.5 Further metal feedstocks

Also for less frequently studied alloy systems in L-PBF, nanoparticulate surface functionalization by dry coating was demonstrated to improve processability and part properties. Li et al. (2019) produced W/ZrC (0.5 wt%) composite powders by coating W microparticles with ZrC nanoparticles in a high energy mill. The composite powder allowed for manufacture of dense parts due to suppression of columnar grain growth. The crack density of W/ZrC components was decreased by 88.7% as compared to those built from pure W feedstock. Zhang et al. (2019) prepared TiAl6V4/SiC (5 wt%) nanocomposite powders for PBF-LB/M by ball milling. Parts produced from this composite showed improved micro hardness, impact strength and less wear as compared to components manufactured from pristine feedstock due to grain refinement and dispersion strengthening via the *in-situ* formation of $TiC/Ti_5Si_3$ upon processing. SiC nanoparticles are also an efficient grain refiner for the Mg alloy AZ91D. Niu et al. (2021) performed coating of AZ91D with SiC in a ball mill and demonstrated that the built components show superior mechanical properties compared to those obtained from non-functionalized feedstock. This is explained by a transition of columnar-to-equiaxed grain growth.

Shuai et al. (2021) dry coated Zn microparticles in a ball mill with CNT@Ag nanoparticles. They showed that a PBF-LB/M-produced implant from this composite powder showed an increased compressive yield strength, ultimate tensile strength, and elongation at break compared to the reference by 22%, 26 % and 17%, respectively. This shows the positive effect of well-dispersed CNTs. Wegner et al. (2021) performed dry coating of a feedstock powder for the formation of Zr-based bulk metallic glasses (AMZ4) with fumed silica in a turbular mixer. Dry coating improves the feedstock's flowability as demonstrated by measurements of the dynamic angle of repose. Here, overdosing of the flowing aid impaired the performance of the obtained components due to incorporation of oxygen impurities in the system and induced partial crystallization.

Nanoparticulate surface functionalization of feedstocks also was exploited to form nano-ceramic surface layers on the built components. Zhou et al. (2018), Zhou et al. (2020a), Zhou et al. (2020b) coated MoTiAl powders coated with $Al_2O_3$ (5 wt%) nanoparticles and CNTs by means of heteroaggregation in the liquid phase. The Mo alloy components were characterized by a ceramic $Al_2O_3$ surface layer providing good corrosion resistance for Mo. Finally, coating of the built layer with TiNi nanoparticles during processing was shown as an approach to fill microcracks and voids leading to improved part properties (Ravichander et al., 2021).

## 4 Conclusion

Dry particle coating for preparation of polymer and metal PBF feedstocks is a highly promising method to improve AM processing. Recent research trends and methods for

characterization of the feedstock's bulk solid properties relevant to AM processability have been reviewed in this contribution. Feedstocks of good flowability and high bulk density are mandatory to assure homogeneously spread powder layers and homogeneous and high packing densities of the feedstock throughout the build volume. These important preconditions are required for production of dense parts of accurate geometries and sufficient mechanical strength. Final component properties are determined to a large extend by the bulk solid characteristics of the used feedstocks. Dry particle coating of polymer particles and (cohesive) metal powders has been demonstrated in various works as a viable approach for preparation of composite particle systems that assure the necessary bulk solid properties for AM processing. More recently, dry particle coating was not only exploited to tune the material's flowability, but also to tailor further relevant materials properties, such as absorptivity and charge formation, or to tune the resulting microstructure of components. These composite powders enhance economic efficiency of the AM process by providing higher built rates. Moreover, dry particle coating was applied to produce 'functional' composite feedstocks for manufacture of e.g. conductive or magnetic parts. The aforementioned efforts for functionalization of PBF feedstocks support process stability, improve component properties via e.g. tuned microstructures, pave the way towards more reliable AM-produced parts for a broad range of applications and open novel pathways to process material systems that so far could not be processed.

Regarding bulk solid characterization, measurements under static conditions and high load, i.e. shear tests, as well as dynamic measurements under free surface conditions are suitable to assess the PBF feedstock's behavior at ambient conditions. Funnel flow tests, measurement of the angle of repose or the Hausner ratio are simple but often insufficient to assess the flowability of PBF feedstocks. These methods, although frequently used and recommended as characterization methods in the norms, are rather insensitive and even may lead to misleading interpretations (Hesse et al., 2021). More advanced and reliable methods include the determination of the avalanche angle during powder spreading experiments, Jenike or Schulze shear tests, measurements in powder rheometers or determination of the bulk solid's compressibility. In particular, polymer feedstock characterization should be performed also at building chamber temperature, as measurements at ambient temperature do not allow for a reliable assessment of the feedstock's behavior under process conditions. Moreover, also the effect of the spreader geometry and the effects of possible jamming during powder spreading should be assessed by powder spreading experiments. This review clearly shows that coating of the feedstocks and comprehensive characterization of the powders requires in-depth knowledge application of fundamentals in particle technology. Only well-designed and fully characterized powder will lead to excellent parts properties in AM.

## Author contributions

JS and WP contributed to the conception and design of this work. Both authors wrote this manuscript and approve the submitted version.

## Funding

This study has been funded by Deutsche Forschungsgemeinschaft (DFG, German Research Foundation) in the framework of CRC814 "Additive Manufacturing" (project-ID 61375930, subproject A1) and PP2122 "Materials for Additive Manufacturing" (grant SCHM3230/1-1, project-ID 409808524).

## Acknowledgments

Financial support by DFG within CRC814 "Additive Manufacturing" and PP2122 "Materials for Additive Manufacturing" is gratefully acknowledged. Furthermore, we acknowledge financial support by Deutsche Forschungsgemeinschaft and Friedrich-Alexander-Universität Erlangen-Nürnberg within the funding program "Open Access Publication Funding".

## Conflict of interest

The authors declare that the research was conducted in the absence of any commercial or financial relationships that could be construed as a potential conflict of interest.

## Publisher's note

All claims expressed in this article are solely those of the authors and do not necessarily represent those of their affiliated organizations, or those of the publisher, the editors and the reviewers. Any product that may be evaluated in this article, or claim that may be made by its manufacturer, is not guaranteed or endorsed by the publisher.

## Supplementary material

The Supplementary Material for this article can be found online at: https://www.frontiersin.org/articles/10.3389/fceng.2022.995221/full#supplementary-material

# References


Alonso, M., Satoh, M., and Miyanami, K. (1988). Powder coating in a rotary mixer with rocking motion. *Powder Technol.* 56, 135–141. doi:10.1016/0032-5910(88)80007-X

Amado, A., Schmid, M., Levy, G., and Wegener, K. (2011). Advances in SLS powder characterization. *SFF Proc.* 2011, 438–452.

Blümel, C. (2015). *Charakterisierung der Trockenen Beschichtung zur Herstellung von maßgeschneiderten Kompositpartikeln*. München: Verl. Dr. Hut. Zugl. Erlangen-Nürnberg, Univ., Diss.

Blümel, C., Sachs, M., Laumer, T., Winzer, B., Schmidt, J., Schmidt, M., et al. (2015). Increasing flowability and bulk density of PE-HD powders by a dry particle coating process and impact on LBM processes. *Rapid Prototyp. J.* 21, 697–704. doi:10.1108/rpj-07-2013-0074

Blümel, C., Schmidt, J., Dielesen, A., Sachs, M., Winzer, B., Peukert, W., et al. (2014). Dry particle coating of polymer particles for tailor-made product properties. *AIP Conf. Proc.* 1593, 248. doi:10.1063/1.4873774

Bose, S., and Bogner, R. H. (2007). Solventless pharmaceutical coating processes: A review. *Pharm. Dev. Technol.* 12, 115–131. doi:10.1080/10837450701212479

Carrozza, A., Saboori, A., Biamino, S., Lombardi, M., Aversa, A., Marchese, G., et al. (2020). "Advanced powder characterization for laser powder-bed fusion of AlSi10Mg," in Euro PM 2018 congress and exhibition,Bilbao, Spain.

Chatham, C. A., Long, T. E., and Williams, C. B. (2019). A review of the process physics and material screening methods for polymer powder bed fusion additive manufacturing. *Prog. Polym. Sci.* 93, 68–95. doi:10.1016/j.progpolymsci.2019.03.003

Chen, B., Davies, R., Liu, Y., Yi, N., Qiang, D., Zhu, Y., et al. (2020). Laser sintering of graphene nanoplatelets encapsulated polyamide powders. *Addit. Manuf.* 35, 101363. doi:10.1016/j.addma.2020.101363

Cho, Y., and Cho, J. (2010). Significant improvement of LiNi[sub 0.8]Co[sub 0.15]Al[sub 0.05]O[sub 2] cathodes at 60°C by SiO[sub 2] dry coating for Li-ion batteries. *J. Electrochem. Soc.* 157, A625. doi:10.1149/1.3363852

Clayton, J., Millington-Smith, D., and Armstrong, B. (2015). The application of powder rheology in additive manufacturing. *JOM* 67, 544–548. doi:10.1007/s11837-015-1293-z

Cordova, L., Campos, M., and Tinga, T. (2019). Revealing the Effects of Powder Reuse for Selective Laser Melting by Powder Characterization. *JOM* 71, 1062. doi:10.1007/s11837-018-3305-2

Cordova, L., Bor, T., de Smit, M., Campos, M., and Tinga, T. (2020). Measuring the spreadability of pre-treated and moisturized powders for laser powder bed fusion. *Addit. Manuf.* 32, 101082. doi:10.1016/j.addma.2020.101082

Dechet, M. A., Goblirsch, A., Romeis, S., Zhao, M., Lanyi, F. J., Kaschta, J., et al. (2019). Production of polyamide 11 microparticles for Additive Manufacturing by liquid-liquid phase separation and precipitation. *Chem. Eng. Sci.* 197, 11–25. doi:10.1016/j.ces.2018.11.051

Dechet, M. A., Gómez Bonilla, J. S., Grünewald, M., Popp, K., Rudloff, J., Lang, M., et al. (2021). A novel, precipitated polybutylene terephthalate feedstock material for powder bed fusion of polymers (PBF): Material development and initial PBF processability. *Mat. Des.* 197, 109265. doi:10.1016/j.matdes.2020.109265

Dechet, M. A., Gómez Bonilla, J. S., Lanzl, L., Drummer, D., Bück, A., Schmidt, J., et al. (2018). Spherical polybutylene terephthalate (PBT)-Polycarbonate (PC) blend particles by mechanical alloying and thermal rounding. *Polym. (Basel)* 10, 1373. doi:10.3390/polym10121373

Doñate-Buendia, C., Kürnsteiner, P., Stern, F., Wilms, M. B., Streubel, R., Kusoglu, I. M., et al. (2021). Microstructure formation and mechanical properties of ODS steels built by laser additive manufacturing of nanoparticle coated iron-chromium powders. *Acta Mater.* 206, 116566. doi:10.1016/j.actamat.2020.116566

Doñate-Buendia, C., Streubel, R., Kürnsteiner, P., Wilms, M. B., Stern, F., Tenkamp, J., et al. (2020). Effect of nanoparticle additivation on the microstructure and microhardness of oxide dispersion strengthened steels produced by laser powder bed fusion and directed energy deposition. *Procedia CIRP* 94, 41–45. doi:10.1016/j.procir.2020.09.009

Düsenberg, B., Kopp, S.-P., Tischer, F., Schrüfer, S., Roth, S., Schmidt, J., et al. (2022a). Enhancing photoelectric powder deposition of polymers by charge control substances. *Polym. (Basel)* 14, 1332. doi:10.3390/polym14071332

Düsenberg, B., Tischer, F., Valayne, E., Schmidt, J., Peukert, W., and Bück, A. (2022b). Temperature influence on the triboelectric powder charging during dry coating of polypropylene with nanosilica particles. *Powder Technol.* 399, 117224. doi:10.1016/j.powtec.2022.117224

Fanselow, S., Emamjomeh, S. E., Wirth, K.-E., Schmidt, J., and Peukert, W. (2016). Production of spherical wax and polyolefin microparticles by melt emulsification for additive manufacturing. *Chem. Eng. Sci.* 141, 282–292. doi:10.1016/j.ces.2015.11.019

Freeman, R. (2007). Measuring the flow properties of consolidated, conditioned and aerated powders — a comparative study using a powder rheometer and a rotational shear cell. *Powder Technol.* 174, 25–33. doi:10.1016/j.powtec.2006.10.016

Gärtner, E., Jung, H. Y., Peter, N. J., Dehm, G., Jägle, E. A., Uhlenwinkel, V., et al. (2021). Reducing cohesion of metal powders for additive manufacturing by nanoparticle dry-coating. *Powder Technol.* 379, 585–595. doi:10.1016/j.powtec.2020.10.065

Gath, C., and Drummer, D. (2016). "Curcuit board application to additive manufactured components by laser-direct-structuring," in 2016 12th International Congress Molded Interconnect Devices - Scientific Proceedings (MID), Wuerzburg, Germany, 28-29 September 2016. doi:10.1109/ICMID.2016.7738926

Ghadiri, M., Pasha, M., Nan, W., Hare, C., Vivacqua, V., Zafar, U., et al. (2020). Cohesive powder flow: Trends and challenges in characterisation and analysis. *KONA Powder Part. J.* 37, 3–18. doi:10.14356/kona.2020018

Gómez Bonilla, J. S., Düsenberg, B., Lanyi, F., Schmuki, P., Schubert, D. W., Schmidt, J., et al. (2021a). Improvement of polymer properties for powder bed fusion by combining *in situ* PECVD nanoparticle synthesis and dry coating. *Plasma process. Polym.* 18, 2000247. doi:10.1002/ppap.202000247

Gomez Bonilla, J. S., Trzenschiok, H., Lanyi, F., Schubert, D. W., Bück, A., Schmidt, J., et al. (2019). "Tailored modification of flow behavior and processability of polypropylene powders in SLS by fluidized bed coating with *in-situ* plasma produced silica nanoparticles," in Solid Freeform Fabrication 2019: Proceedings of the 30th Annual International Solid Freeform Fabrication Symposium - An Additive Manufacturing Conference, Austin, Texas, USA, August 12-14, 2019.

Gómez Bonilla, J. S., Unger, L., Schmidt, J., Peukert, W., and Bück, A. (2021b). Particle Lagrangian CFD simulation and experimental characterization of the rounding of polymer particles in a downer reactor with direct heating. *Processes* 9, 916. doi:10.3390/pr9060916

Götzinger, M., and Peukert, W. (2004). Particle adhesion force distributions on rough surfaces. *Langmuir* 20, 5298–5303. doi:10.1021/la049914f

Guo, C., Yu, Z., Liu, C., Li, X., Zhu, Q., and Mark Ward, R. (2020). Effects of Y2O3 nanoparticles on the high-temperature oxidation behavior of IN738LC manufactured by laser powder bed fusion. *Corros. Sci.* 171, 108715. doi:10.1016/j.corsci.2020.108715

Han, Q., Gu, Y., Setchi, R., Lacan, F., Johnston, R., Evans, S. L., et al. (2019). Additive manufacturing of high-strength crack-free Ni-based Hastelloy X superalloy. *Addit. Manuf.* 30, 100919. doi:10.1016/j.addma.2019.100919

Han, Q., Gu, Y., Wang, L., Feng, Q., Gu, H., Johnston, R., et al. (2020). Effects of TiC content on microstructure and mechanical properties of nickel-based hastelloy X nanocomposites manufactured by selective laser melting. *Mater. Sci. Eng. A* 796, 140008. doi:10.1016/j.msea.2020.140008

Heiland, S., Milkereit, B., Hoyer, K.-P., Zhuravlev, E., Kessler, O., and Schaper, M. (2021). Requirements for processing high-strength alznmgcu alloys with pbf-lb/m to achieve crack-free and dense parts. *Materials* 14, 7190. doi:10.3390/ma14237190

Hesse, N., Winzer, B., Peukert, W., and Schmidt, J. (2021). Towards a generally applicable methodology for the characterization of particle properties relevant to processing in powder bed fusion of polymers – from single particle to bulk solid behavior. *Addit. Manuf.* 41, 101957. doi:10.1016/j.addma.2021.101957

Hupfeld, T., Doñate-Buendía, C., Krause, M., Sommereyns, A., Wegner, A., Sinnemann, T., et al. (2020a). Scaling up colloidal surface additivation of polymer powders for laser powder bed fusion. *Procedia CIRP* 94, 110–115. doi:10.1016/j.procir.2020.09.022

Hupfeld, T., Salamon, S., Landers, J., Sommereyns, A., Doñate-Buendía, C., Schmidt, J., et al. (2020b). 3D printing of magnetic parts by laser powder bed fusion of iron oxide nanoparticle functionalized polyamide powders. *J. Mat. Chem. C Mat.* 8, 12204–12217. doi:10.1039/d0tc02740e

Hupfeld, T., Sommereyns, A., Riahi, F., Doñate-Buendía, C., Gann, S., Schmidt, M., et al. (2020c). Analysis of the nanoparticle dispersion and its effect on the crystalline microstructure in carbon-additivated PA12 feedstock material for laser powder bed fusion. *Materials* 13, 3312. doi:10.3390/ma13153312

Hupfeld, T., Sommereyns, A., Schuffenhauer, T., Zhuravlev, E., Krebs, M., Gann, S., et al. (2020d). *How colloidal surface additivation of polyamide 12 powders with well-dispersed silver nanoparticles influences the crystallization already at low 0.01 vol%*, 36. doi:10.1016/j.addma.2020.101419*Addit. Manuf.*

Israelachvili, J. N. (2011). *Intermolecular and surface forces*. Burlington, MA: Academic Press.

Jadhav, S. D., Dadbakhsh, S., Chen, R., Shabadi, R., Kruth, J.-P., van Humbeeck, J., et al. (2020). Modification of electrical and mechanical properties of selective laser-melted CuCr0.3 alloy using carbon nanoparticles. *Adv. Eng. Mat.* 22, 1900946. doi:10.1002/adem.201900946

Jadhav, S. D., Dadbakhsh, S., Vleugels, J., Hofkens, J., Puyvelde, P. V., Yang, S., et al. (2019). Influence of carbon nanoparticle addition (and impurities) on selective laser melting of pure copper. *Materials* 12, 2469. doi:10.3390/ma12152469

Jadhav, S. D., Dhekne, P. P., Brodu, E., van Hooreweder, B., Dadbakhsh, S., Kruth, J.-P., et al. (2021). Laser powder bed fusion additive manufacturing of highly conductive parts made of optically absorptive carburized CuCr1 powder. *Mat. Des.* 198, 109369. doi:10.1016/j.matdes.2020.109369

Jenike, A. W. (1964). *Storage and flow of solids: Bulletin No. 123 of the Utah engineering experimentall section*. Salt Lake City, UT: University of Utah.

Karg, M. C. H., Munk, A., Ahuja, B., Backer, M. V., Schmitt, J. P., Stengel, C., et al. (2019). Expanding particle size distribution and morphology of aluminium-silicon powders for Laser Beam Melting by dry coating with silica nanoparticles. *J. Mater. Process. Technol.* 264, 155–171. doi:10.1016/j.jmatprotec.2018.08.045

Karg, M. C. H., Rasch, M., Schmidt, K., Spitzer, S. A. E., Karsten, T. F., Schlaug, D., et al. (2018). Laser alloying advantages by dry coating metallic powder mixtures with SiOx nanoparticles. *Nanomaterials* 8, 862. doi:10.3390/nano8100862

Kaye, B. H., Gratton-Liimatainen, J., and Faddis, N. (1995). Studying the avalanching behaviour of a powder in a rotating disc. *Part. Part. Syst. Charact.* 12, 232–236. doi:10.1002/ppsc.19950120505

Kenel, C., de Luca, A., Joglekar, S. S., Leinenbach, C., and Dunand, D. C. (2021). Evolution of Y2O3 dispersoids during laser powder bed fusion of oxide dispersion strengthened Ni-Cr-Al-Ti γ/γ' superalloy. *Addit. Manuf.* 47, 102224. doi:10.1016/j.addma.2021.102224

Kleijnen, R. G., Schmid, M., and Wegener, K. (2019). "Impact of flow aid on the flowability and coalescence of polymer laser sintering powder," in Solid Freeform Fabrication 2019: Proceedings of the 30th Annual International Solid Freeform Fabrication Symposium - An Additive Manufacturing Conference, Austin, Texas, USA, August 12-14, 2019.

Kloos, S., Dechet, M. A., Peukert, W., and Schmidt, J. (2018). Production of spherical semi-crystalline polycarbonate microparticles for Additive Manufacturing by liquid-liquid phase separation. *Powder Technol.* 335, 275–284. doi:10.1016/j.powtec.2018.05.005

Krantz, M., Zhang, H., and Zhu, J. (2009). Characterization of powder flow: Static and dynamic testing. *Powder Technol.* 194, 239–245. doi:10.1016/j.powtec.2009.05.001

Krinitcyn, M., Toropkov, N., Pervikov, A., Glazkova, E., and Lerner, M. (2021). Characterization of nano / micro bimodal 316L SS powder obtained by electrical explosion of wire for feedstock application in powder injection molding. *Powder Technol.* 394, 225–233. doi:10.1016/j.powtec.2021.08.061

Kusoglu, I. M., Gökce, B., and Barcikowski, S. (2020). Use of (nano-)additives in Laser Powder Bed Fusion of Al powder feedstocks: Research directions within the last decade. *Procedia CIRP* 94, 11–16. doi:10.1016/j.procir.2020.09.003

Kusoglu, I. M., Huber, F., Doñate-Buendía, C., Rosa Ziefuss, A., Gökce, B., T Sehrt, J., et al. (2021). Nanoparticle additivation effects on laser powder bed fusion of metals and polymers-A theoretical concept for an inter-laboratory study design all along the process chain, including research data management. *Mater. (Basel)* 14, 4892. doi:10.3390/ma14174892

Larsson, S., Gustafsson, G., Oudich, A., Jonsén, P., and Häggblad, H. (2016). Experimental methodology for study of granular material flow using digital speckle photography. *Chemical Engineering Science* 155, 524. doi:10.1016/j.ces.2016.09.010

Leturia, M., Benali, M., Lagarde, S., Ronga, I., and Saleh, K. (2014). Characterization of flow properties of cohesive powders: A comparative study of traditional and new testing methods. *Powder Technol.* 253, 406–423. doi:10.1016/j.powtec.2013.11.045

Lexow, M. M., and Drummer, D. (2016). New materials for SLS: The use of antistatic and flow agents. *J. Powder Technol.* 2016, 1–9. doi:10.1155/2016/4101089

Li, K., Wang, D., Xing, L., Wang, Y., Yu, C., Chen, J., et al. (2019). Crack suppression in additively manufactured tungsten by introducing secondary-phase nanoparticles into the matrix. *Int. J. Refract. Metals Hard Mater.* 79, 158–163. doi:10.1016/j.ijrmhm.2018.11.013

Li, X., Li, G., Zhang, M.-X., and Zhu, Q. (2021). Novel approach to additively manufacture high-strength Al alloys by laser powder bed fusion through addition of hybrid grain refiners. *Addit. Manuf.* 48, 102400. doi:10.1016/j.addma.2021.102400

Linsenbühler, M., and Wirth, K.-E. (2005). An innovative dry powder coating process in non-polar liquids producing tailor-made micro-particles. *Powder Technol.* 158, 3–20. doi:10.1016/j.powtec.2005.04.035

Lüddecke, A., Pannitz, O., Zetzener, H., Sehrt, J. T., and Kwade, A. (2021). Powder properties and flowability measurements of tailored nanocomposites for powder bed fusion applications. *Mat. Des.* 202, 109536. doi:10.1016/j.matdes.2021.109536

Lyckfeldt, O. (2013). "Powder rheology of steel powders for additive manufacturing," in International powder metallurgy congress and exhibition Trento, Italy. Euro PM 2013.

Mair, P., Goettgens, V. S., Rainer, T., Weinberger, N., Letofsky-Papst, I., Mitsche, S., et al. (2021). Laser powder bed fusion of nano-CaB6 decorated 2024 aluminum alloy. *J. Alloys Compd.* 863, 158714. doi:10.1016/j.jallcom.2021.158714

Mair, P., Kaserer, L., Braun, J., Stajkovic, J., Klein, C., Schimbäck, D., et al. (2022). Dependence of mechanical properties and microstructure on solidification onset temperature for Al2024–CaB6 alloys processed using laser powder bed fusion. *Mater. Sci. Eng. A* 833, 142552. doi:10.1016/j.msea.2021.142552

Mellin, P., Lyckfeldt, O., Harlin, P., Brodin, H., Blom, H., and Strondl, A. (2017). Evaluating flowability of additive manufacturing powders, using the Gustavsson flow meter. *Metal. Powder Rep.* 72, 322–326. doi:10.1016/j.mprp.2017.06.003

Minasyan, T., and Hussainova, I. (2022). Laser powder-bed fusion of ceramic particulate reinforced aluminum alloys: A review. *Mater. (Basel)* 15, 2467. doi:10.3390/ma15072467

Naito, M., Kondo, A., and Yokoyama, T. (1993). Applications of comminution techniques for the surface modification of powder materials. *ISIJ Int.* 33, 915–924. doi:10.2355/isijinternational.33.915

Nan, W., Pasha, M., Bonakdar, T., Lopez, A., Zafar, U., Nadimi, S., et al. (2018). Jamming during particle spreading in additive manufacturing. *Powder Technol.* 338, 253–262. doi:10.1016/j.powtec.2018.07.030

Niu, X., Shen, H., Fu, J., and Feng, J. (2021). Effective control of microstructure evolution in AZ91D magnesium alloy by SiC nanoparticles in laser powder-bed fusion. *Mat. Des.* 206, 109787. doi:10.1016/j.matdes.2021.109787

Pannitz, O., Großwendt, F., Lüddecke, A., Kwade, A., Röttger, A., and Sehrt, J. T. (2021). Improved process efficiency in laser-based powder bed fusion of nanoparticle coated maraging tool steel powder. *Materials* 14, 3465. doi:10.3390/ma14133465

Paul, B. K., Lee, K., He, Y., Ghayoor, M., Chang, C.-H., and Pasebani, S. (2020). Oxide dispersion strengthened 304 L stainless steel produced by ink jetting and laser powder bed fusion. *CIRP Ann.* 69, 193–196. doi:10.1016/j.cirp.2020.04.071

Pazos, D., Cintins, A., de Castro, V., Fernández, P., Hoffmann, J., Vargas, W. G., et al. (2018). ODS ferritic steels obtained from gas atomized powders through the STARS processing route: Reactive synthesis as an alternative to mechanical alloying. *Nucl. Mater. Energy* 17, 1–8. doi:10.1016/j.nme.2018.06.014

Pfeffer, R., Dave, R. N., Wei, D., and Ramlakhan, M. (2001). Synthesis of engineered particulates with tailored properties using dry particle coating. *Powder Technol.* 117, 40–67. doi:10.1016/S0032-5910(01)00314-X

Pleass, C., and Jothi, S. (2018). Influence of powder characteristics and additive manufacturing process parameters on the microstructure and mechanical behaviour of Inconel 625 fabricated by Selective Laser Melting. *Addit. Manuf.* 24, 419–431. doi:10.1016/j.addma.2018.09.023

Qu, M., Guo, Q., Escano, L. I., Nabaa, A., Hojjatzadeh, S. M. H., Young, Z. A., et al. (2022). Controlling process instability for defect lean metal additive manufacturing. *Nat. Commun.* 13, 1079. doi:10.1038/s41467-022-28649-2

Ravichander, B. B., Amerinatanzi, A., and Moghaddam, N. S. (2021). Toward mitigating microcracks using nanopowders in laser powder bed fusion. *Proc. SPIE - Int. Soc. Opt. Eng.* 11589. doi:10.1117/12.2585606

Ruggi, D., Barrès, C., Charmeau, J.-Y., Fulchiron, R., Barletta, D., and Poletto, M. (2020). A quantitative approach to assess high temperature flow properties of a PA 12 powder for laser sintering. *Addit. Manuf.* 33, 101143. doi:10.1016/j.addma.2020.101143

Rumpf, H. (1974). Die Wissenschaft des Agglomerierens. *Chem. Ing. Techn.* 46, 1–11. doi:10.1002/cite.330460102

Sachs, M., Friedle, M., Schmidt, J., Peukert, W., and Wirth, K.-E. (2017). Characterization of a downer reactor for particle rounding. *Powder Technol.* 316, 357–366. doi:10.1016/j.powtec.2017.01.006

Sachs, M., Schmidt, J., Peukert, W., and Wirth, K.-E. (2018). Treatment of polymer powders by combining an atmospheric plasma jet and a fluidized bed reactor. *Powder Technol.* 325, 490–497. doi:10.1016/j.powtec.2017.11.016

Schmid, M., Amado, A., and Wegener, K. (2015). Polymer powders for selective laser sintering (SLS). *AIP Conf. Proc.* 1664, 160009. doi:10.1063/1.4918516

Schmid, M. (2018). *Laser sintering with plastics: Technology, processes, and materials*. Cincinnati, Munich: Hanser Publishers.

Schmidt, J., Dechet, M. A., Gómez Bonilla, J. S., Hesse, N., Bück, A., and Peukert, W. (2019b). "Characterization of polymer powders for selective laser sintering," in Solid Freeform Fabrication 2019: Proceedings of the 30th Annual International

Solid Freeform Fabrication Symposium - An Additive Manufacturing Conference, Austin, Texas, USA, August 12-14, 2019.

Schmidt, J., Dechet, M., Bonilla, J. G., Kloos, S., Wirth, K. E., and Peukert, W. (2019a). Novel process routes towards the production of spherical polymer powders for selective laser sintering. *AIP Conf. Proc.* 2139. doi:10.1063/1.5121697

Schmidt, J., Parteli, E. J. R., Uhlmann, N., Wörlein, N., Wirth, K.-E., Pöschel, T., et al. (2020). Packings of micron-sized spherical particles – insights from bulk density determination, X-ray microtomography and discrete element simulations. *Adv. Powder Technol.* 31, 2293–2304. doi:10.1016/j.apt.2020.03.018

Schmidt, J., Plata, M., Tröger, S., and Peukert, W. (2012). Production of polymer particles below 5 µm by wet grinding. *Powder Technol.* 228, 84–90. doi:10.1016/j.powtec.2012.04.064

Schmidt, J., Sachs, M., Blümel, C., Winzer, B., Toni, F., Wirth, K.-E., et al. (2015). A novel process chain for the production of spherical sls polymer powders with good flowability. *Procedia Eng.* 102, 550–556. doi:10.1016/j.proeng.2015.01.123

Schmidt, J., Sachs, M., Blümel, C., Winzer, B., Toni, F., Wirth, K.-E., et al. (2014). A novel process route for the production of spherical LBM polymer powders with small size and good flowability. *Powder Technol.* 261, 78–86. doi:10.1016/j.powtec.2014.04.003

Schmidt, J., Sachs, M., Fanselow, S., Wirth, K.-E., and Peukert, W. (2017). New approaches towards production of polymer powders for selective laser beam melting of polymers. *AIP Conf. Proc.* 1914, 190008. doi:10.1063/1.5016797

Schmidt, J., Sachs, M., Fanselow, S., Wirth, K.-E., and Peukert, W. (2016a). "Novel approaches for the production of polymer powders for selective laser beam melting of polymers," in Solid Freeform Fabrication 2016: Proceedings of the 27th Annual International Solid Freeform Fabrication Symposium - An Additive Manufacturing Conference, Austin, Texas, USA, August 12-14, 2019.

Schmidt, J., Sachs, M., Fanselow, S., Zhao, M., Romeis, S., Drummer, D., et al. (2016b). Optimized polybutylene terephthalate powders for selective laser beam melting. *Chem. Eng. Sci.* 156, 1–10. doi:10.1016/j.ces.2016.09.009

Schmidt, J., Sachs, M., Zhao, M., Fanselow, S., Wudy, K., Drexler, M., et al. (2016c). A novel process for production of spherical PBT powders and their processing behavior during laser beam melting. *AIP Conf. Proc.* 1713. doi:10.1063/1.4942343

Schulze, D. (2008). *Powders and bulk solids: Behavior, characterization, storage and flow*. Berlin: Springer.

Schwedes, J. (2003). Review on testers for measuring flow properties of bulk solids. *Granul. Matter* 5, 1–43. doi:10.1007/s10035-002-0124-4

Sehrt, J. T., Kleszczynski, S., and Notthoff, C. (2017). Nanoparticle improved metal materials for additive manufacturing. *Prog. Addit. Manuf.* 2, 179–191. doi:10.1007/s40964-017-0028-9

Shad, A., Stache, R., and Rütjes, A. (2021). Effects of fumed silica flow aids on flowability and packing of metal powders used in Binder-Jetting additive manufacturing process. *Mat. Des.* 212, 110253. doi:10.1016/j.matdes.2021.110253

Shen, J., Li, Z., Li, H., Yao, B., and Teng, B. (2022). Additive manufacturing of high relative density Cu-0.8Cr alloy by low power 1064 nm Yb-fiber laser powder bed fusion: Role of Nano-TiC modification. *Mater. Lett.* 308, 131141. doi:10.1016/j.matlet.2021.131141

Shuai, C., Dong, Z., Yang, W., He, C., Yang, Y., and Peng, S. (2021). Rivet-inspired modification of carbon nanotubes by *in situ*-reduced Ag nanoparticles to enhance the strength and ductility of Zn implants. *ACS Biomater. Sci. Eng.* 7, 5484–5496. doi:10.1021/acsbiomaterials.1c00931

Sommereyns, A., Gann, S., Schmidt, J., Chehreh, A. B., Lüddecke, A., Walther, F., et al. (2021a). Quality over quantity: How different dispersion qualities of minute amounts of nano-additives affect material properties in powder bed fusion of polyamide 12. *Materials* 14, 5322. doi:10.3390/ma14185322

Sommereyns, A., Hupfeld, T., Gann, S., Wang, T., Wu, C., Zhuravlev, E., et al. (2021b). Influence of sub-monolayer quantities of carbon nanoparticles on the melting and crystallization behavior of polyamide 12 powders for additive manufacturing. *Mat. Des.* 201, 109487. doi:10.1016/j.matdes.2021.109487

Spierings, A. B., Voegtlin, M., Bauer, T., and Wegener, K. (2016). Powder flowability characterisation methodology for powder-bed-based metal additive manufacturing. *Prog. Addit. Manuf.* 1, 9–20. doi:10.1007/s40964-015-0001-4

Sun, J., Zhang, B., and Qu, X. (2021). High strength Al alloy development for laser powder bed fusion. *J. Micromech. Mol. Phys.* 6. doi:10.1142/S2424913021410010

Tan, Q., Zhang, J., Mo, N., Fan, Z., Yin, Y., Bermingham, M., et al. (2020). A novel method to 3D-print fine-grained AlSi10Mg alloy with isotropic properties via inoculation with LaB6 nanoparticles. *Addit. Manuf.* 32, 101034. doi:10.1016/j.addma.2019.101034

Tan, Y., Zhang, J., Li, X., Xu, Y., and Wu, C.-Y. (2021). Comprehensive evaluation of powder flowability for additive manufacturing using principal component analysis. *Powder Technol.* 393, 154–164. doi:10.1016/j.powtec.2021.07.069

Tertuliano, O. A., DePond, P. J., Doan, D., Matthews, M. J., Gu, X. W., Cai, W., et al. (2022). Nanoparticle-enhanced absorptivity of copper during laser powder bed fusion. *Addit. Manuf.* 51, 102562. doi:10.1016/j.addma.2021.102562

Tischer, F., Düsenberg, B., Gräser, T., Kaschta, J., Schmidt, J., and Peukert, W. (2022). Abrasion-induced acceleration of melt crystallisation of wet comminuted polybutylene terephthalate (PBT). *Polym. (Basel)* 14, 810. doi:10.3390/polym14040810

Tomas, J., and Kleinschmidt, S. (2009). Improvement of flowability of fine cohesive powders by flow additives. *Chem. Eng. Technol.* 32, 1470–1483. doi:10.1002/ceat.200900173

Vieth, P., Voigt, M., Ebbert, C., Milkereit, B., Zhuravlev, E., Yang, B., et al. (2020). Surface inoculation of aluminium powders for additive manufacturing of Al-7075 alloys. *Procedia CIRP* 94, 17–20. doi:10.1016/j.procir.2020.09.004

Vock, S., Klöden, B., Kirchner, A., Weißgärber, T., and Kieback, B. (2019). Powders for powder bed fusion: A review. *Prog. Addit. Manuf.* 4, 383–397. doi:10.1007/s40964-019-00078-6

Wang, Y., and Shi, J. (2020). Effect of hot isostatic pressing on nanoparticles reinforced AlSi10Mg produced by selective laser melting. *Mater. Sci. Eng. A* 788, 139570. doi:10.1016/j.msea.2020.139570

Wegner, J., Frey, M., Piechotta, M., Neuber, N., Adam, B., Platt, S., et al. (2021). Influence of powder characteristics on the structural and the mechanical properties of additively manufactured Zr-based bulk metallic glass. *Mat. Des.* 209, 109976. doi:10.1016/j.matdes.2021.109976

Wu, W., Gao, C., Liu, Z., Wong, K., and Xiao, Z. (2021). Laser powder bed fusion of crack-free TiN/Al7075 composites with enhanced mechanical properties. *Mater. Lett.* 282, 128625. doi:10.1016/j.matlet.2020.128625

Xi, S., Zhang, P., Huang, Y., Kong, M., Yang, Q., and Li, G. (2020). Laser sintering of cryogenically ground polymer powders into high-performance parts: The role of dry particle coating with a conductive flow agent. *Polymer* 186, 122044. doi:10.1016/j.polymer.2019.122044

Xinwei, L., Shi, S., Shuang, H., Xiaogang, H., Qiang, Z., Hongxing, L., et al. (2020). Microstructure, solidification behavior and mechanical properties of Al-Si-Mg-Ti/TiC fabricated by selective laser melting. *Addit. Manuf.* 34, 101326. doi:10.1016/j.addma.2020.101326

Yang, J., Sliva, A., Banerjee, A., Dave, R. N., and Pfeffer, R. (2005). Dry particle coating for improving the flowability of cohesive powders. *Powder Technol.* 158, 21–33. doi:10.1016/j.powtec.2005.04.032

Yang, Y., Doñate-Buendía, C., Oyedeji, T. D., Gökce, B., and Xu, B.-X. (2021). Nanoparticle tracing during laser powder bed fusion of oxide dispersion strengthened steels. *Materials* 14, 3463. doi:10.3390/ma14133463

Yao, X., Moon, S. K., Lee, B. Y., and Bi, G. (2017). Effects of heat treatment on microstructures and tensile properties of IN718/TiC nanocomposite fabricated by selective laser melting. *Int. J. Precis. Eng. Manuf.* 18, 1693–1701. doi:10.1007/s12541-017-0197-y

Yazdani, B., Chen, B., Benedetti, L., Davies, R., Ghita, O., and Zhu, Y. (2018). A new method to prepare composite powders customized for high temperature laser sintering. *Compos. Sci. Technol.* 167, 243–250. doi:10.1016/j.compscitech.2018.08.006

Yokoyama, T., Urayama, K., Naito, M., Kato, M., and Yokoyama, T. (1987). The angmill mechanofusion system and its applications. *KONA* 5, 59–68. doi:10.14356/kona.1987011

Zhai, W., Zhou, W., Nai, S. M. L., and Wei, J. (2020). Characterization of nanoparticle mixed 316 L powder for additive manufacturing. *J. Mat. Sci. Technol.* 47, 162–168. doi:10.1016/j.jmst.2020.02.019

Zhang, X., Mao, B., Histed, R., Trabia, M., O'Toole, B., Jennings, R., et al. (2019). "Selective laser melting of Ti/SiC nanocomposite coating towards enhanced surface performance of Ti64," in MS and T 2019 - materials science and Technology, Portland, Oregon. doi:10.7449/2019/MST_2019_356_363

Zhou, H., Götzinger, M., and Peukert, W. (2003). The influence of particle charge and roughness on particle–substrate adhesion. *Powder Technol.* 135-136, 82–91. doi:10.1016/j.powtec.2003.08.007

Zhou, H., and Peukert, W. (2008). Modeling adhesion forces between deformable bodies by FEM and Hamaker summation. *Langmuir* 24, 1459–1468. doi:10.1021/la7023023

Zhou, W., Kikuchi, K., Nomura, N., Yoshimi, K., and Kawasaki, A. (2020a). *In-situ* formation of ceramic layer on Mo-based composites via laser powder bed fusion. *Materialia* 10, 100655. doi:10.1016/j.mtla.2020.100655

Zhou, W., Kikuchi, K., Nomura, N., Yoshimi, K., and Kawasaki, A. (2020b). Novel laser additive-manufactured Mo-based composite with enhanced mechanical and oxidation properties. *J. Alloys Compd.* 819, 152981. doi:10.1016/j.jallcom.2019.152981

Zhou, W., Sun, X., Kikuchi, K., Nomura, N., Yoshimi, K., and Kawasaki, A. (2018). Carbon nanotubes as a unique agent to fabricate nanoceramic/metal composite powders for additive manufacturing. *Mat. Des.* 137, 276–285. doi:10.1016/j.matdes.2017.10.034

Zhou, W., Zhu, G., Wang, R., Yang, C., Tian, Y., Zhang, L., et al. (2020c). Inhibition of cracking by grain boundary modification in a non-weldable nickel-based superalloy processed by laser powder bed fusion. *Mater. Sci. Eng. A* 791, 139745. doi:10.1016/j.msea.2020.139745

Zhuravlev, E., Milkereit, B., Yang, B., Heiland, S., Vieth, P., Voigt, M., et al. (2021). Assessment of AlZnMgCu alloy powder modification for crack-free laser powder bed fusion by differential fast scanning calorimetry. *Mater. Des.* 204, 109677. doi:10.1016/j.matdes.2021.109677

Ziegelmeier, S., Christou, P., Wöllecke, F., Tuck, C., Goodridge, R., Hague, R., et al. (2015). An experimental study into the effects of bulk and flow behaviour of laser sintering polymer powders on resulting part properties. *J. Mater. Process. Technol.* 215, 239–250. doi:10.1016/j.jmatprotec.2014.07.029

Ziegelmeier, S., Wöllecke, F., Tuck, C., Goodridge, R., and Hague, R. (2013). "Characterizing the bulk & flow behaviour of LS polymer powders," in SFF Symposium 2013, Austin, TX, 354–367.

Zimmermann, I., Eber, M., and Meyer, K. (2004). Nanomaterials as flow regulators in dry powders. *Z. für Phys. Chem.* 218, 51–102. doi:10.1524/zpch.218.1.51.25388